

**Solution-Phase Synthesis of the Fluorogenic TGase 2 Acyl Donor Z-Glu(HMC)-Gly-OH and its Use for Inhibitor and Amine Substrate Characterisation**

Wodtke, R.; Pietsch, M.; Löser, R.;

Originally published:

February 2020

**Analytical Biochemistry 595(2020), 113612**

DOI: <https://doi.org/10.1016/j.ab.2020.113612>

Perma-Link to Publication Repository of HZDR:

<https://www.hzdr.de/publications/Publ-30151>

Release of the secondary publication  
on the basis of the German Copyright Law § 38 Section 4.

CC BY-NC-ND

# Solution-Phase Synthesis of the Fluorogenic TGase 2 Acyl Donor Z-Glu(HMC)-Gly-OH and its Use for Inhibitor and Amine Substrate Characterisation

Robert Wodtke <sup>1\*</sup>, Markus Pietsch <sup>2</sup> and Reik Löser <sup>1,3\*</sup>

<sup>1</sup> Helmholtz-Zentrum Dresden-Rossendorf, Institute of Radiopharmaceutical Cancer Research; Bautzner Landstrasse 400, 01328 Dresden, Germany

<sup>2</sup> Institute II of Pharmacology, Centre of Pharmacology, Medical Faculty, University of Cologne, Gleueler Strasse 24, 50931 Cologne, Germany

<sup>3</sup> Faculty of Chemistry and Food Chemistry, School of Science, Technische Universität Dresden, Mommsenstraße 4, 01062 Dresden, Germany

**Abstract:** A reliable solution-phase synthesis of the water-soluble dipeptidic fluorogenic transglutaminase substrate Z-Glu(HMC)-Gly-OH is presented. The route started from Z-Glu-OH, which was converted into the corresponding cyclic anhydride. This building block was transformed into the regioisomeric  $\alpha$ - and  $\gamma$ -dipeptides. The key step was the esterification of Z-Glu-Gly-OtBu with 4-methylumbelliferone. The final substrate compound was obtained in an acceptable yield and excellent purity without the need of purification by RP-HPLC. The advantage of this acyl donor substrate for the kinetic characterisation of inhibitors and amine-type acyl acceptor substrates is demonstrated by evaluating commercially available or literature-known irreversible inhibitors and the biogenic amines serotonin, histamine and dopamine, respectively.

**Keywords:** fluorogenic enzyme substrates; side-chain esterified peptides; aryl esters; peptide synthesis; enzyme kinetics; biogenic amines

## 1. Introduction

Transglutaminase 2 is a multifunctional enzyme whose distinct physiological roles are incompletely understood [1, 2]. Its eponymous and best-characterised function represents the catalysis of the acyl transfer between glutamine residues and a variety of primary amines [3]. To assess the significance of this enzymatic activity in cells, substrates (especially low molecular weight polyamines) [4, 5] and inhibitors [6] were applied amongst other biochemical techniques [7, 8]. The prerequisite for an accurate interpretation of potential effects mediated by those TGase 2-targeting molecules is the knowledge of their kinetic properties towards the isolated protein and also towards

---

\*Correspondence: [r.wodtke@hzdr.de](mailto:r.wodtke@hzdr.de), [r.loeser@hzdr.de](mailto:r.loeser@hzdr.de); Tel.: +49-351-260-3658

## Abbreviations

d...doublet, DIPEA...*N,N*-diisopropylethylamine, EDTA...*N,N'*-ethylenediamine tetraacetic acid, GDH...glutamate dehydrogenase, hTGase 2...human TGase 2; HMC...7-hydroxy-4-methylcoumarin (=4-methylumbelliferone), HATU...(1-[bis(dimethylamino)methylene]-1*H*-1,2,3-triazolo[4,5-*b*]pyridinium 3-oxide hexafluorophosphate, HPLC...high performance liquid chromatography, Hsp...heat shock protein, LC...liquid chromatography, m...multiplet, MES... 2-(*N*-morpholino)ethanesulfonic acid, MOPS...(3-(*N*-morpholino)propanesulfonic acid), MS...mass spectrometry, NMM...*N*-methylmorpholine, NMR...nuclear magnetic resonance, Np...4-nitrophenyl, PyBOP...benzotriazol-1-yl-oxytripyrrolidinophosphonium hexafluorophosphate, q...quadruplet, RP...reversed phase, s...singlet, t...triplet, TCEP...tris(2-carboxyethyl)phosphine, TLC...thin layer chromatography, UPLC...Ultra Performance Liquid Chromatography, Z...benzyloxycarbonyl (=carbobenzoy, Cbz); all other abbreviations are in accordance to the recommendations of the IUPAC-IUB commission on biochemical nomenclature, see Eur. J. Biochem. 15 (1970) 203-208 and Eur. J. Biochem. 138 (1984) 9-37

the other members of the transglutaminase family. The other main function of TGase 2 is dealing with the binding of GDP and GTP and catalysis of hydrolysis of the latter [9]. Both functions are mutually exclusive as they are associated with distinct conformational states of the enzyme molecule [10]. Therefore, occupation of the guanine nucleotide binding site of TGase 2 can be analysed via detection of its acyltransferase activity [11, 12], which indicates the value of robust assay methods that allow for the monitoring of this activity [13]. A rigorous kinetic assessment of the enzyme's acyltransferase activity is enabled by the dipeptidic coumarinyl ester Z-Glu(HMC)-Gly-OH as fluorogenic substrate. In addition to its suitable kinetic and spectral properties, the compound's utility is owed to its propitious water solubility [14]. Favourably, this compound can be also used for the assay of other transglutaminase isoforms [15]. The synthesis of peptides containing glutamate coumarinyl esters was achieved by solid-phase peptide synthesis using the chlorotriyl linker for attachment to the solid support. The ester moiety in the glutamate side-chain was installed after deblocking the allyl ester-protected  $\gamma$ -carboxylic acid function prior to acidic cleavage from the resin [14]. Although this synthesis strategy is advantageous for obtaining various peptidic substrates, the product scale is limited by the use of the costly polymeric resin and the need of preparative RP-HPLC for purification. Efficient solution-phase methods have been described by Chung *et al.* [16] and Leblanc *et al.* [17] for the synthesis of the corresponding chromogenic dipeptidic substrate Z-Glu(ONp)-Gly-OH, which bears a nitrophenyl group attached to the identical peptidic scaffold. This pathway was adopted by us for an efficient access to Z-Glu(HMC)-Gly-OH, which will be reported herein together with its kinetic evaluation towards TGase 2-catalysed hydrolysis. In this context, it was envisaged to re-prove the fluorogenic substrate's previously established value for TGase 2 inhibitor and substrate characterisation exemplarily for commercially available irreversible inhibitors for which robust second-order inactivation constants  $k_{\text{inact}}/K_i$  have not been reported so far. Furthermore, kinetic parameters for selected physiologically relevant amine substrates were determined by taking advantage of the title compound.

## 2. Materials and Methods

### 2.1. General

All starting materials, reagents and solvents were commercially obtained and used without further purification. Compound **5**, *N*-monodansylpiperazine and *N*-acryloxysuccinimide were synthesised as previously published [15]. Chromatographic separations and TLC detections were carried out with Merck Silica Gel 60 (63–200  $\mu\text{m}$ ) and Merck Silica Gel 60 F<sub>254</sub> sheets, respectively. TLCs were visualised under UV light ( $\lambda = 254 \text{ nm}$  or  $365 \text{ nm}$ ). Analytical RP-HPLC was carried out with a system consisting of a Merck Hitachi L7100 gradient pump combined with a Jasco DG2080 four-line degasser with UV detection with a Merck Hitachi L7450 diode array detector. The system was operated with D-700 HSM software and use of a Merck Hitachi D7000 interface. A Luna C18 5  $\mu\text{m}$  column (Phenomenex, 250 $\times$ 4.6 mm) served as stationary phase. A binary gradient system of 0.1% CF<sub>3</sub>COOH/water (solvent A) and 0.1% CF<sub>3</sub>COOH/CH<sub>3</sub>CN (solvent B) at a flow rate of 1 mL/min served as the eluent. The following elution programme was run to separate the components: 0–3 min 80% A, 3–45 min gradient to 70% B, 45–46 min gradient to 95% B, 46–50 min 95% B, 50–55 min gradient back to 80% A, 55–60 min 80% A. For purification of compound **7**, preparative HPLC were performed on a Varian Prepstar system equipped with a UV detector (Prostar, Varian). A Microsorb C18 60–8 column (Varian Dynamax 250 mm  $\times$  21.4 mm) was used as the stationary phase. The same binary gradient system as for the analytical RP-HPLC was applied using an appropriate gradient from low to high percentage of B with a slope of 1% per min.

Melting points were determined on a Galen III Boetius apparatus from Cambridge Instruments. NMR spectra were recorded on a Varian Unity 400 MHz or an Agilent DD2 600 MHz spectrometer equipped with ProbeOne probe. Chemical shifts of the <sup>1</sup>H and <sup>13</sup>C spectra were reported in parts per million (ppm) referenced to the (residual) solvent resonances relative to tetramethylsilane. UPLC-MS was performed on a Waters ACQUITY UPLC I-Class system including an ACQUITY UPLC PDA e $\lambda$

setector coupled to a Xevo TQ-S mass spectrometer High-resolution mass spectra were obtained on an Agilent UHD Accurate-Mass Q-TOF LC MS G6538A mass spectrometer operated in combination with coupled with the Agilent 1260 Infinity II HPLC system. Elemental microanalysis was performed on a Euro EA 3000 Elemental Analyzer (Euro Vector Instruments & Software).

## 2.2. Benzyl (S)-(2,6-dioxotetrahydro-2H-pyran-3-yl)carbamate (**1**, N-Carbobenzoxylglutamic anhydride)

Z-Glu-OH (2.5 g, 8.89 mmol) was suspended in acetic anhydride (20 mL) and the temperature was slowly raised to 55 °C (oil bath temperature), whereupon a clear solution was formed. From the time of complete dissolution, stirring was continued for additional 10 min. The solution was concentrated under high vacuum (rotary evaporator equipped with hybrid vacuum pump) to obtain a nearly colourless oil. Ether (30 mL) was added to the crude product and ethyl acetate (5-10 mL) was added until a homogeneous solution was obtained upon heating. The solution was transferred to an Erlenmeyer flask and cyclohexane (15-20 mL) was added until the solution became turbid. The mixture was kept at -20 °C over night, whereupon an oil separated. Crystallisation was initiated by scratching with a glass rod. More cyclohexane (10 mL) was added and the mixture was kept again at -20 °C over night. The crystalline material was collected by vacuum filtration and dried *in vacuo* to obtain **1** (2.1 g, 0.80 mmol, 90%) as a white powder; Mp 82-86 °C (lit 86-88 °C [18]); <sup>1</sup>H NMR (400 MHz, CDCl<sub>3</sub>), δ (ppm): 1.94 (qd, <sup>2</sup>J=13.1 Hz, <sup>3</sup>J=5.6 Hz, 1H, C<sub>β</sub>-HH), 2.45-2.59 (m, 1H, C<sub>β</sub>-HH), 2.90 (ddd, <sup>2</sup>J=18.9 Hz, <sup>3</sup>J=13.0 Hz, <sup>3</sup>J=6.2 Hz, 1H, C<sub>γ</sub>-HH), 3.06 (ddd, <sup>2</sup>J=18.7 Hz, <sup>3</sup>J=5.6 Hz, <sup>3</sup>J=2.2 Hz, 1H, C<sub>γ</sub>-HH), 4.38-4.52 (m, 1H, C<sub>α</sub>-H), 5.15 (s, 2H, CH<sub>2</sub>O), 5.57 (br s, 1H, NH), 7.30-7.42 (m, 5H, Ph-H); <sup>13</sup>C NMR (100 MHz, CDCl<sub>3</sub>), δ (ppm): 23.72 (C<sub>β</sub>), 29.83 (C<sub>γ</sub>), 51.48 (C<sub>α</sub>), 67.77 (CH<sub>2</sub>O), 128.39, 128.64, 128.80, 135.80, (C<sub>arom</sub>), 155.81, OCONH), 164.53, 166.65 (2×C=O anhydride). NMR data are in agreement to those reported in [17]. Elemental analysis C<sub>13</sub>H<sub>13</sub>NO<sub>5</sub>, calcd. C: 59.31%, H: 4.98%, N: 5.32%, found: C: 58.33%, H: 5.15%, N: 5.16%.

## 2.3. (S)-4-(((Benzyloxy)carbonyl)amino)-5-((2-(tert-butoxy)-2-oxoethyl)amino)-5-oxopentanoic acid (**2**, Z-Glu-Gly-OtBu)

To a solution of compound **1** (0.5 g, 1.90 mmol) in chloroform (20 mL) was added glycine *tert*-butyl ester hydrochloride (H-Gly-OtBu×HCl; 0.32 g, 1.90 mmol) as a solid followed by triethyl amine (0.19 g, 0.26 mL, 1.90 mmol). The resulting solution was stirred for 30 min at room temperature. The solvent was removed *in vacuo* and the obtained crude product mixture was adsorbed on silica gel and loaded onto a silica column. Product **2** was obtained by elution with ether/ethyl acetate/acetic acid 1:1:0.01. As the UV absorption of both products is rather low, visualisation of compound spots during monitoring of the chromatographic purification by TLC analysis of distinct fractions was done by using Hanessian's stain [19]. The product-containing fraction were combined and brought to dryness *in vacuo*. The obtained oily residue was crystallised by dissolving in a minimum amount of ethyl acetate and subsequent addition of a larger volume of cyclohexane. The oil which separated from the solvent mixture solidified at -20 °C. The solid was collected by vacuum filtration to obtain 373 mg (50 %) of compound **2**. R<sub>f</sub> 0.35 (*n*-hexane/ethyl acetate/acetic acid 1:4:0.01); Mp 96-103 °C (lit 106- 107 °C [20]); <sup>1</sup>H NMR (400 MHz, CDCl<sub>3</sub>), δ (ppm): 1.45 (s, 9H, (CH<sub>3</sub>)<sub>3</sub>C), 1.88 – 2.01 (m, 1H, C<sub>β</sub>-HH), 2.09 – 2.20 (m, 1H, C<sub>β</sub>-HH), 2.41 – 2.59 (m, 2H, C<sub>γ</sub>-H<sub>2</sub>), 3.83 – 4.00 (m, 2H, <sup>Gly</sup>C<sub>α</sub>-H<sub>2</sub>), 4.41 – 4.49 (m, 1H, <sup>Glu</sup>C<sub>α</sub>-H), 5.05-5.17 (m, 2H, CH<sub>2</sub>O), 5.88 (d, <sup>3</sup>J=8.6 Hz, 1H, Glu-NH), 7.10-7.16 (br s, 1H, Gly-NH), 7.27-7.39 (m, 5H, Ph-H); <sup>13</sup>C NMR (100 MHz, CDCl<sub>3</sub>), δ (ppm): 28.16 (3×CH<sub>3</sub>), 28.28 (C<sub>β</sub>), 29.91 (C<sub>γ</sub>), 42.25 (<sup>Gly</sup>C<sub>α</sub>), 53.85 (<sup>Glu</sup>C<sub>α</sub>), 67.44 (CH<sub>2</sub>O), 82.75 ((CH<sub>3</sub>)<sub>3</sub>C), 128.20, 128.37, 128.68, 136.14 (4×C<sub>arom</sub>), 156.70 (OCONH), 169.06, 171.93, 176.71 (3×C=O). NMR data are in agreement to those reported in [17]. Elemental analysis C<sub>19</sub>H<sub>26</sub>N<sub>2</sub>O<sub>7</sub>: calcd. C: 57.86%, H: 6.64%, N: 7.10%, found: C: 58.97%, H: 6.79%, N: 6.94%.

## 2.4. N<sup>2</sup>-((Benzyloxy)carbonyl)-N<sup>5</sup>-(2-(tert-butoxy)-2-oxoethyl)-L-glutamine (**2a**)

Compound **2a** was obtained by further elution of the chromatographic column described above with ether/ethyl acetate/acetic acid 1:4:0.01. The product-containing fractions were combined and

brought to dryness *in vacuo*. The obtained oily residue was washed with cyclohexane under ultrasonification to remove residual acetic acid, which was followed by washing with *n*-pentane. The oil was dried under very low pressure (< 0.1 mbar) to obtain 223 mg (30%) of compound **2a** as a white foam.  $R_f$  0.17 (*n*-hexane/ethyl acetate/acetic acid 1:4:0.01);  $^1\text{H}$  NMR (400 MHz,  $\text{CDCl}_3$ )  $\delta$  (ppm): 1.45 (s, 9H,  $(\text{CH}_3)_3\text{C}$ ), 1.99 – 2.09 (m, 1H,  $\text{C}_\beta\text{-HH}$ ), 2.15 – 2.27 (m,  $\text{C}_\beta\text{-HH}$ , 1H), 2.30 – 2.49 (m, 2H,  $\text{C}_\gamma\text{-H}_2$ ), 3.84 – 3.96 (m, 2H,  $\text{GlyC}_\alpha\text{-H}_2$ ), 4.32 – 4.43 (m, 1H,  $\text{GluC}_\alpha\text{-H}$ ), 5.08 (s, 2H,  $\text{CH}_2\text{O}$ ), 6.02 (d,  $^3J=7.5$  Hz, 1H, Glu-NH), 6.77 (t,  $^3J=4.9$  Hz, 1H, Gly-NH), 7.27 – 7.35 (m, 5H, Ph-H),  $^{13}\text{C}$  NMR (100 MHz,  $\text{CDCl}_3$ )  $\delta$  (ppm): 28.12 ( $3\times\text{CH}_3$ ), 28.50 ( $\text{C}_\beta$ ), 32.13 ( $\text{C}_\gamma$ ), 42.35 ( $\text{GlyC}_\alpha$ ), 53.48 ( $\text{GluC}_\alpha$ ), 67.24 ( $\text{CH}_2\text{O}$ ), 82.91 ( $(\text{CH}_3)_3\text{C}$ ), 128.19, 128.31, 128.65, 136.28 ( $4\times\text{C}_{\text{arom}}$ ), 156.61 (OCONH), 169.39, 173.61, 174.34 ( $3\times\text{C=O}$ ). Elemental analysis  $\text{C}_{19}\text{H}_{26}\text{N}_2\text{O}_7$ : calcd. C: 57.86%, H: 6.64%, N: 7.10%, found: C: 57.36%, H: 6.74%, N: 6.58%.

#### 2.5. 4-Methyl-2-oxo-2H-chromen-7-yl (S)-4-(((benzyloxy)carbonyl)amino)-5-((2-(tert-butoxy)-2-oxoethyl)amino)-5-oxopentanoate (3, Z-Glu(HMC)-Gly-OtBu)

Compound **2** (0.373 g, 0.95 mmol) and HATU (0.361 g, 0.95 mmol) were dissolved in DMF (3 mL) under a  $\text{N}_2$  atmosphere. DIPEA (282  $\mu\text{L}$ , 1.88 mmol) and a solution of 4-methylumbelliferone (0.168 g, 0.95 mmol) in DMF (1 mL) were added to this mixture. The resulting yellow solution was stirred for 2 h at room temperature. Subsequently, the solution was diluted with  $\text{CH}_2\text{Cl}_2$  (15 mL), transferred to a separatory funnel and washed with 1 M HCl (1 $\times$ 3 mL), sat.  $\text{NaHCO}_3$  (2 $\times$ 3 mL),  $\text{H}_2\text{O}$  (1 $\times$ 3 mL) and brine (1 $\times$ 1 mL). The organic layer was dried over  $\text{Na}_2\text{SO}_4$  and evaporated *in vacuo* (the remaining DMF was removed using a rotary evaporator equipped with hybrid pump for very low pressure) to obtain a yellow viscous oil. The crude product was purified by column chromatography on silica gel using a mixture of *n*-hexane and ethyl acetate of increasing polarity (ratio starting from 6:4 over 1:1 to 4:6; the final ratio was adjusted 20 fractions after unconverted 4-methylumbelliferone eluted). The product-containing fractions were collected and evaporated *in vacuo* to obtain 243 mg of compound **3** as an off-white solid. As the product still contained 4-methylumbelliferone as trace impurity, the material was recrystallised by adding ethyl acetate (3.2 mL) to a refluxing suspension of the product in cyclohexane (4 mL). Upon keeping the solution at 4  $^\circ\text{C}$  overnight, a precipitate was formed, which was collected by vacuum filtration, washed with cyclohexane and *n*-hexane and dried *in vacuo* to obtain compound **3** (134 mg, 26%) as a white granulous solid.  $R_f$  0.16 (*n*-hexane/ethyl acetate 1:1); Mp 61–63  $^\circ\text{C}$ ;  $^1\text{H}$  NMR (400 MHz,  $\text{CDCl}_3$ )  $\delta$  (ppm): 1.47 (s, 9H,  $(\text{CH}_3)_3\text{C}$ ), 2.02 – 2.14 (m, 1H,  $\text{C}_\beta\text{-HH}$ ), 2.26–2.38 (m, 1H,  $\text{C}_\beta\text{-HH}$ ), 2.43 (d,  $^4J=1.3$  Hz, 3H,  $\text{CH}_3\text{-coumarin}$ ), 2.67–2.90 (m, 2H,  $\text{C}_\gamma\text{-H}_2$ ), 3.90 (dd,  $^2J=18.2$  Hz,  $^3J=5.1$  Hz, 1H,  $\text{C}_\alpha\text{-HH}$  of Gly), 3.98 (dd,  $^2J=18.3$  Hz,  $^3J=5.4$  Hz, 1H,  $\text{C}_\alpha\text{-HH}$  of Gly), 4.37 – 4.44 (m, 1H,  $\text{C}_\alpha\text{-H}$  of Glu) 5.11 (d,  $^2J=12.3$  Hz, 1H,  $\text{CHHO}$ ), 5.15 (d,  $^2J=12.9$  Hz, 1H,  $\text{CHHO}$ ), 5.58 (d,  $^3J=8.0$  Hz, 1H, Glu-NH), 6.27 (q,  $^4J=1.3$  Hz, 1H, H-3 of coumarin), 6.51 (br s, 1H, Gly-NH) 7.07 – 7.11 (m, 1H, H-6 of coumarin), 7.13 (d,  $^4J=1.8$  Hz, 1H, H-8 of coumarin), 7.28 – 7.38 (m, 5H, Ph-H), 7.57 (d,  $^3J=8.6$  Hz, 1H, H-5 of coumarin).  $^{13}\text{C}$  NMR (100 MHz,  $\text{CDCl}_3$ )  $\delta$  (ppm): 18.88 ( $\text{CH}_3$  of coumarin), 28.20 ( $3\times\text{CH}_3$ ), 28.30 ( $\text{C}_\beta$ ), 30.52 ( $\text{C}_\gamma$ ), 42.18 ( $\text{C}_\alpha$  of Gly), 53.92 ( $\text{C}_\alpha$  of Glu), 67.43 ( $\text{CH}_2\text{O}$ ), 82.75 ( $(\text{CH}_3)_3\text{C}$ ), 110.65 (C8 of coumarin), 114.76 (C3 of coumarin), 118.09, 118.27 (C4a and C6 of coumarin), 125.53 (C5 of coumarin), 128.30, 128.42, 128.73 ( $3\times\text{CH}$  of phenyl), 136.18 (C1 of phenyl), 151.99, 153.10, 154.34 (C4, C7 and C8a of coumarin), 156.37 (OCONH), 160.61 (C2 of coumarin), 168.62, 171.00, 171.54 ( $3\times\text{C=O}$ ). HR-MS (ESI $^+$ ):  $[\text{M}+\text{NH}_4]^+$  calculated: 570.2451, found: 570.2445 (90%),  $[\text{2M}+\text{NH}_4]^+$  calculated: 1122.4559, found: 1122.4565 (100%). Elemental analysis  $\text{C}_{29}\text{H}_{32}\text{N}_2\text{O}_9$ : calcd. C: 63.04%, H: 5.84%, N: 5.07%, found: C: 62.48%, H: 5.82%, N: 4.73%.

#### 2.6. (S)-2-(((Benzyloxy)carbonyl)amino)-5-((4-methyl-2-oxo-2H-chromen-7-yl)oxy)-5-oxopentanoylglycine (4, Z-Glu(HMC)-Gly-OH)

To a solution of compound **3** (130 mg, 0.24 mmol) in  $\text{CH}_2\text{Cl}_2$  (0.5 mL) was added slowly trifluoroacetic acid (4 mL) under ice cooling. After stirring for 2 h under ice cooling the solvents were removed under a  $\text{N}_2$  stream under ambient pressure. The oily residue was taken up into  $\text{CH}_2\text{Cl}_2$  (20 mL) and washed with 0.1 M HCl (5 mL). As addition of HCl resulted in the formation of an emulsion, brine (3 mL) was added, whereupon a white precipitate was formed, which was filtered off and

redissolved in ethyl acetate (15 mL). The aqueous layer was separated from the combined biphasic mixture and the organic layer was dried over Na<sub>2</sub>SO<sub>4</sub> and evaporated *in vacuo* to obtain 112 mg of a white solid. Since an impurity was detectable in the <sup>1</sup>H NMR spectrum, the crude product was recrystallised. To this end, the solid was dissolved in a mixture of ethyl acetate (4 mL) and acetonitrile (2 mL) under heating. Cyclohexane (6 mL) was added and the resulting solution was kept at 4 °C for 30 min, whereupon a gelatinous precipitate formed. The material was collected by vacuum filtration, washed with cyclohexane and *n*-pentane and dried *in vacuo* to obtain compound **4** (77 mg, 65%) as a white solid. R<sub>f</sub> 0.01 (*n*-hexane/ethyl acetate 2:8); Mp 167–171 °C; <sup>1</sup>H NMR (400 MHz, DMSO-*d*<sub>6</sub>) δ (ppm): 1.88–1.98 (m, 1H, C<sub>β</sub>-HH), 2.02–2.14 (m, 1H, C<sub>β</sub>-HH), 2.44 (d, <sup>4</sup>J=1.3 Hz, 3H, CH<sub>3</sub>-coumarin), 2.68–2.75 (m, 2H, C<sub>γ</sub>-H<sub>2</sub>), 3.73 (dd, <sup>2</sup>J=17.5, <sup>3</sup>J=5.6 Hz, 1H, C<sub>α</sub>-HH of Gly), 3.83 (dd, <sup>2</sup>J=17.5, <sup>3</sup>J=6.0 Hz, 1H, C<sub>α</sub>-HH of Gly), 4.15–4.21 (m, 1H, C<sub>α</sub>-H of Glu), 5.02 (d, <sup>2</sup>J=12.6 Hz, 1H, CHHO), 5.07 (d, <sup>2</sup>J=12.6 Hz, 1H, CHHO), 6.39 (d, <sup>4</sup>J=1.3 Hz, 1H, H-3 of coumarin), 7.18 (dd, <sup>3</sup>J=8.7, 2.3 Hz, 1H, H-6 of coumarin), 7.26 (d, <sup>4</sup>J=2.3 Hz, 1H, H-8 of coumarin), 7.28–7.39 (m, 5H, Ph-H), 7.54 (d, <sup>3</sup>J=8.3 Hz, 1H, Glu-NH), 7.81 (d, <sup>3</sup>J=8.7 Hz, 1H, H-5 of coumarin), 8.29 (t, <sup>3</sup>J=5.8 Hz, 1H, Gly-NH). <sup>13</sup>C NMR (100 MHz, CDCl<sub>3</sub>) δ (ppm): 18.11 (CH<sub>3</sub> of coumarin), 26.98 (C<sub>β</sub>), 30.00 (C<sub>γ</sub>), 40.66 (C<sub>α</sub> of Gly), 53.49 (C<sub>α</sub> of Glu), 65.51 (CH<sub>2</sub>O), 110.04 (C8 of coumarin), 113.69 (C3 of coumarin), 117.47 (C4a of coumarin), 118.34 (C6 of coumarin), 126.32 (C5 of coumarin), 127.66, 127.74, 128.27 (3×CH of phenyl), 136.88 (C1 of phenyl), 152.82, 152.90, 153.48 (C4, C7 and C8a of coumarin), 155.92 (OCONH), 159.55 (C2 of coumarin), 170.82, 171.03, 171.51 (3×C=O). NMR data are in agreement to those reported in [14]. HR-MS (ESI+): *m/z* calculated for [M+NH<sub>4</sub>]<sup>+</sup>: 514.1825, found: 514.1821 (100%), [2M+NH<sub>4</sub>]<sup>+</sup>: calculated: 1010.3307, found: 1010.3313 (57.2%), [3M+NH<sub>4</sub>]<sup>+</sup>: calculated: 1506.4789, found: 1506.4799 (80.52%). Elemental analysis: C<sub>25</sub>H<sub>24</sub>N<sub>2</sub>O<sub>9</sub>·H<sub>2</sub>O calcd. C: 58.36%, H: 5.09%, N: 5.45%, found: C: 58.36%, H: 4.92%, N: 5.23%. Chromatograms for UPLC-MS analysis of Z-Glu(HMC)-Gly-OH (**4**) are shown in Figure S2 (Supporting Information).

## 2.7. tert-Butyl (2-(4-((5-(dimethylamino)naphthalen-1-yl)sulfonyl)piperazin-1-yl)-2-oxoethyl)carbamate (**6a**, N-Boc-glycine-4-dansylpiperazide)

To a solution of Boc-glycine (98.8 mg, 0.56 mmol) and DIPEA (196.5 μL, 0.12 mmol) in DMF (5 mL) was added PyBOP (293 mg, 0.56 mmol). The solution was stirred for 5 min at room temperature and, subsequently, N-monodansylpiperazine (90 mg, 0.28 mmol) was added. After stirring for 3 h, the solvent of the reaction mixture was removed *in vacuo* and the obtained residue was dissolved in ethyl acetate (15 mL). The organic phase was washed with sat. NaHCO<sub>3</sub> (2×10 mL) and brine (1×10 mL), dried over Na<sub>2</sub>SO<sub>4</sub> and evaporated to dryness. The obtained crude product was subjected to column chromatography (silica; eluent: petroleum ether/ethyl acetate (25 → 50%)) to obtain **6a** (133 mg, 100%) as a light-green solid; <sup>1</sup>H NMR (400 MHz, CDCl<sub>3</sub>): δ=1.41 (s, 9H, 3×CH<sub>3</sub> of Boc), 2.90 (s, 6H, 2×CH<sub>3</sub> of dansyl), 3.23–3.15 (m, 4H, 2×CH<sub>2</sub> of piperazine), 3.45–3.39 (m, 2H, CH<sub>2</sub> of piperazine), 3.69–3.62 (m, 2H, CH<sub>2</sub> of piperazine), 3.86 (d, <sup>3</sup>J=4.5 Hz, 2H, CH<sub>2</sub> Gly), 5.36 (br s, NH), 7.21 (d, <sup>3</sup>J=7.5 Hz, 1H, H<sub>Dansyl</sub>), 7.55 (dd, <sup>3</sup>J=8.6, 7.6 Hz, 2H, 2×H<sub>Dansyl</sub>), 8.20 (dd, <sup>3</sup>J=7.3 Hz, <sup>4</sup>J=1.2 Hz, 1H, H<sub>Dansyl</sub>), 8.37 (d, <sup>3</sup>J=8.7 Hz, 1H, H<sub>Dansyl</sub>), 8.59 (d, <sup>3</sup>J=8.5 Hz, 1H, H<sub>Dansyl</sub>); <sup>13</sup>C NMR (100 MHz, CDCl<sub>3</sub>): δ=28.45 (3×CH<sub>3</sub> Boc), 41.68 (CH<sub>2</sub> of piperazine), 42.28 (CH<sub>2</sub> of Gly), 44.24 (CH<sub>2</sub> of piperazine), 45.48 (CH<sub>2</sub> of piperazine), 45.63 (CH<sub>2</sub> of piperazine), 45.65 (2×CH<sub>3</sub> dansyl), 80.03 (C<sub>quartär</sub> of Boc), 115.67, 119.65, 123.45, 128.45, 130.16 (C<sub>quart</sub> of dansyl), 130.44 (C<sub>quart</sub> of dansyl), 131.03, 131.16, 132.30 (C<sub>quart</sub> of dansyl), 151.68 (C<sub>quart</sub> of dansyl), 155.87 (CO of Boc), 167.07; MS (ESI+) 477.3 ([M+H]<sup>+</sup>). <sup>1</sup>H and <sup>13</sup>C NMR spectra in agreement to published data [21].

## 2.8. 2-Amino-1-(4-((5-(dimethylamino)naphthalen-1-yl)sulfonyl)piperazin-1-yl)ethan-1-one (**6b**, Glycine-4-dansylpiperazide)

Compound **6a** (167 mg, 0.35 mmol) was dissolved in a mixture of TFA and CH<sub>2</sub>Cl<sub>2</sub> (10 mL; 1:1, v/v) and stirred for 2 h at room temperature. The volatiles were removed at ambient pressure in a nitrogen stream. The residue was dissolved in sat. NaHCO<sub>3</sub> (20 mL) and extracted with CH<sub>2</sub>Cl<sub>2</sub> (5×5 mL). The organic phase was dried over Na<sub>2</sub>SO<sub>4</sub> and subsequently evaporated to dryness to

obtain **6b** (131 mg, 100%) as a light-green solid;  $^1\text{H}$  NMR (400 MHz,  $\text{DMSO}-d_6$ ):  $\delta$ =2.83 (s, 6H,  $2\times\text{CH}_3$  of dansyl), 3.12–3.05 (m, 4H,  $2\times\text{CH}_2$  of piperazine), 3.53–3.20 (m, 6H,  $2\times\text{CH}_2$  of piperazine,  $\text{CH}_2$  Gly), 7.27 (d,  $^3J$ =7.5 Hz, 1H,  $\text{H}_{\text{Dansyl}}$ ), 7.70–7.59 (m, 2H,  $2\times\text{H}_{\text{Dansyl}}$ ), 8.13 (dd,  $^3J$ =7.4 Hz,  $^4J$ =1.2 Hz, 1H,  $\text{H}_{\text{Dansyl}}$ ), 8.30 (d,  $^3J$ =8.7 Hz, 1H,  $\text{H}_{\text{Dansyl}}$ ), 8.53 (d,  $^3J$ =8.5 Hz, 1H,  $\text{H}_{\text{Dansyl}}$ ), signal for  $\text{NH}_2$  not detectable;  $^{13}\text{C}$  NMR (100 MHz,  $\text{DMSO}-d_6$ ):  $\delta$ =40.89 ( $\text{CH}_2$  of piperazine), 42.53 ( $\text{CH}_2$  Gly), 43.39 ( $\text{CH}_2$  of piperazine), 45.04 ( $2\times\text{CH}_3$  of dansyl), 45.37 ( $2\times\text{CH}_2$  of piperazine), 115.33, 118.86, 123.70, 129.20 ( $\text{C}_{\text{quart}}$  of dansyl), 129.62 ( $\text{C}_{\text{quart}}$  of dansyl), 130.06, 130.39, 132.48 ( $\text{C}_{\text{quart}}$  of dansyl), 151.42 ( $\text{C}_{\text{quart}}$  of dansyl), 171.55 (CO); MS (ESI+) 377.2 ( $[\text{M}+\text{H}]^+$ )  $^1\text{H}$  and  $^{13}\text{C}$  NMR spectra are in agreement to published data [21].

## 2.9. N-(2-(4-((5-(Dimethylamino)naphthalen-1-yl)sulfonyl)piperazin-1-yl)-2-oxoethyl)acrylamide (**7**, N-Acryloylglycine-4-dansylpiperazide)

To a solution of compound **6b** (112 mg, 0.30 mmol) and TEA (82.5  $\mu\text{L}$ , 0.60 mmol) in  $\text{CH}_2\text{Cl}_2$  (10 mL) was added N-acryloxysuccinimide (50.3 mg, 0.30 mmol) as solid. After 1 h, the same amount of N-acryloxysuccinimide was added again and the mixture was stirred for additional 1 h at room temperature. The solution was washed with sat.  $\text{NaHCO}_3$  ( $2\times 10\text{ mL}$ ), brine ( $1\times 10\text{ mL}$ ); dried over  $\text{Na}_2\text{SO}_4$  and evaporated to dryness. The crude product was purified by preparative RP-HPLC to obtain **7** (10.9 mg, 7%) as a white solid;  $^1\text{H}$  NMR (400 MHz,  $\text{CDCl}_3$ ):  $\delta$ =3.01 (s, 6H,  $2\times\text{CH}_3$  of dansyl), 3.27–3.18 (m, 4H,  $2\times\text{CH}_2$  of piperazine), 3.52–3.45 (m, 2H,  $\text{CH}_2$  of piperazine), 3.72–3.66 (m, 2H,  $\text{CH}_2$  of piperazine), 4.08 (d,  $^3J$ =4.2 Hz, 2H,  $\text{CH}_2$  Gly), 5.68 (dd,  $^3J$ =10.2 Hz,  $^2J$ =1.4 Hz, 1H,  $\text{CH}=\text{CHH}$ ), 8.62 (d,  $^3J$ =8.6 Hz, 1H,  $\text{H}_{\text{Dansyl}}$ ), 6.15 (dd,  $^3J$ =17.0, 10.2 Hz, 1H,  $\text{CH}=\text{CH}_2$ ), 6.28 (dd,  $^3J$ =17.0 Hz,  $^2J$ =1.4 Hz, 1H,  $\text{CH}=\text{CHH}$ ), 6.74 (bs, 1H,  $\text{NH}$  of Gly), 7.31 (d,  $^3J$ =7.6 Hz, 1H,  $\text{H}_{\text{Dansyl}}$ ), 7.64–7.56 (m, 2H,  $2\times\text{H}_{\text{Dansyl}}$ ), 8.24 (dd,  $^3J$ =7.4 Hz,  $^4J$ =1.1 Hz, 1H,  $\text{H}_{\text{Dansyl}}$ ), 8.48 (d,  $^3J$ =8.7 Hz, 1H,  $\text{H}_{\text{Dansyl}}$ ), 8.62 (d,  $^3J$ =8.6 Hz, 1H,  $\text{H}_{\text{Dansyl}}$ );  $^{13}\text{C}$  NMR (100 MHz,  $\text{CDCl}_3$ ):  $\delta$ =41.38 ( $\text{CH}_2$  of Gly), 41.86 ( $\text{CH}_2$  of piperazine), 44.36 ( $\text{CH}_2$  of piperazine), 45.41 ( $\text{CH}_2$  of piperazine), 45.59 ( $\text{CH}_2$  of piperazine), 45.84 ( $2\times\text{CH}_3$  of dansyl), 116.22, 121.07, 124.15, 127.71 ( $\text{CH}=\text{CH}_2$ ), 128.30, 129.57 ( $\text{C}_{\text{quart}}$  of dansyl), 130.01 ( $\text{CH}=\text{CH}_2$ ), 130.43 ( $\text{C}_{\text{quart}}$  of dansyl), 130.57, 131.26, 132.59 ( $\text{C}_{\text{quart}}$  of dansyl), 149.58 ( $\text{C}_{\text{quart}}$  of dansyl), 165.92, 166.56.  $^1\text{H}$  and  $^{13}\text{C}$  NMR spectra in agreement to published data [21].

## 2.10. General assay procedure and analysis

All measurements were conducted at 30  $^\circ\text{C}$  over 900 s (interval of 8 or 10 s) using a Cytation 5 Microplate Reader (BioTek Instruments) and black 96-well microplates with  $\mu\text{CLEAR}^\circledR$  bottom (greiner bio-one). Fluorescence was detected in bottom read mode and predefined settings for excitation ( $360\pm 20\text{ nm}$ ) and emission ( $450\pm 20\text{ nm}$ ) of 7-HMC were chosen. Measurements at pH=8.0 and pH=6.5 were conducted with a sensitivity of 45 and 50, respectively. The assay mixture (200  $\mu\text{L}$ ) contained 190  $\mu\text{L}$  aqueous solution and 10  $\mu\text{L}$  DMSO (5% v/v). The following three buffer systems were used: assay buffer I (100 mM MES, 3 mM  $\text{CaCl}_2$ , 50  $\mu\text{M}$  EDTA, adjusted to pH 6.5 with 1 M NaOH), assay buffer II (100 mM MOPS, 3 mM  $\text{CaCl}_2$ , 50  $\mu\text{M}$  EDTA, adjusted to pH 8.0 with 1 M NaOH) and enzyme buffer (100 mM MOPS, 3 mM  $\text{CaCl}_2$ , 10 mM TCEP, 20% (v/v) glycerol). The buffers were stored at 0  $^\circ\text{C}$  for periods of up to 2 weeks and freshly prepared after that period. The concentration of the hTGase 2 stock solution was 1 mg/mL. All regression analyses were accomplished using GraphPad Prism (version 8.2.1, August 20, 2019). To provide values of mean and SEM, the respective regression analyses were separately accomplished for each experiment and the obtained fit values were collected and statistically analysed. hTGase 2 (T022) and inhibitors Z006 and Z013 were purchased from Zedira (Darmstadt, Germany).

Detailed descriptions of the assay procedures and the kinetic analyses for the characterisation of Z-Glu(HMC)-Gly-OH (**4**) towards enzymatic hydrolysis at pH 6.5 and 8.0 as well as for the kinetic characterisation of amines and irreversible inhibitors are given in recent publications of our group [14, 15]. In brief, the recorded time courses of type  $(\text{RFU}-\text{RFU}_0)=f(t)$  for the enzymatic and spontaneous conversion were analysed by nonlinear (one-phase association) and linear regressions to the experimental data. Subsequently, initial rates  $V_{0\text{total}}$  (in the presence of enzyme) and  $V_{0\text{control}}$  (spontaneous reaction in the absence of enzyme) were derived. Both data sets were globally analysed

by applying the model of total and nonspecific binding (implemented in GraphPad Prism) to obtain the kinetic parameters for the enzymatic reaction. According to that model, the following rule was defined:

$$v_{0\text{total}}(\text{enzymatic} + \text{spontaneous}) = v_{0\text{corr}}(\text{enzymatic}) + v_{0\text{control}}(\text{spontaneous}) \quad (1)$$

where  $v_{0\text{corr}}$  represents the rates for the enzymatic conversions (without spontaneous reaction). The spontaneous and enzymatic conversions are mathematically defined within this model by the following equations:

$$v_{0\text{control}} = k_{\text{obs}} * [\text{S}] \quad (2)$$

$$v_{0\text{corr}} = \frac{v_{\text{max}} * [\text{S}]}{K_{\text{m}} + [\text{S}]} \quad (3)$$

Accordingly,  $v_{0\text{total}}$  is defined by the sum function of equations (2) and (3). Due to negligible spontaneous reaction of **4** at pH 6.5, the above mentioned rule simplifies as follows:

$$v_{0\text{total}} = v_{0\text{corr}} \quad (4)$$

However, concerning the kinetic analyses the previously published procedures were slightly adjusted, as detailed below.

Concerning the enzymatic hydrolysis of Z-Glu(HMC)-Gly-OH (**4**) at pH 6.5, the recorded time courses of type  $(\text{RFU}-\text{RFU}_0)=f(t)$  were analysed by either nonlinear (one-phase association) or linear regression over the entire measurement period of 900 s (instead of only the first 300 s) to the experimental data depending on the shape of the curve.

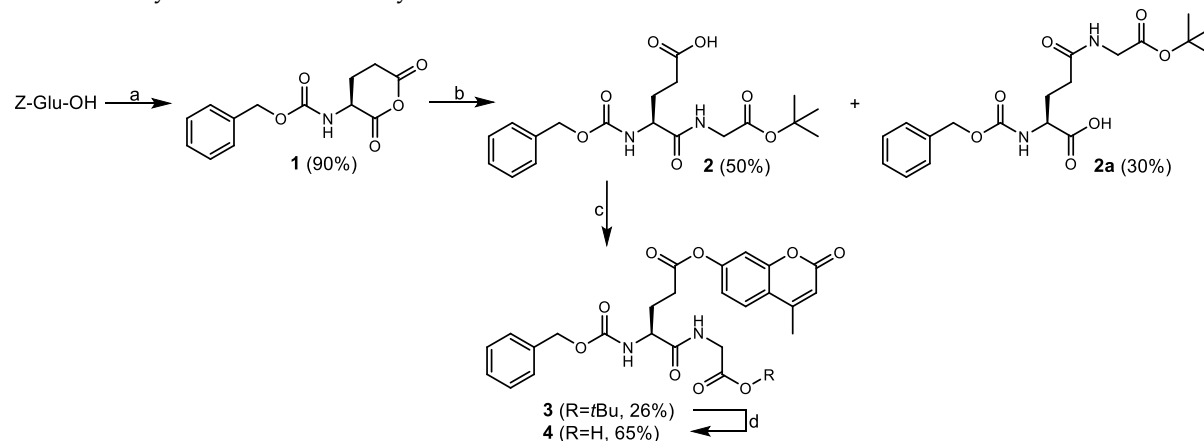
Concerning the kinetic characterisation of the biogenic amines, the two sets of initial rates ( $v_{0\text{total}}=f([\text{amine}])$  and  $v_{0\text{control}}=f([\text{amine}])$ ) were also globally analysed using the model of total and nonspecific binding (instead of simple subtraction of  $v_{0\text{control}}$  from  $v_{0\text{total}}$  values) as conducted for the analysis of the enzymatic hydrolyses).

### 3. Results and Discussion

The four-step synthesis started from commercially available Z-Glu-OH and the first two steps followed mainly the procedures published by Leblanc *et al.* [17] (Scheme 1). Treatment of Z-Glu-OH with acetic anhydride, which acts both as solvent and condensation agent, at elevated temperature led to the corresponding cyclic anhydride **1**. The oily crude product obtained by concentration of the reaction mixture could be crystallised by treatment with ether, ethyl acetate and cyclohexane (see Material and Methods section), which resulted in an almost quantitative yield of 90%. From a historical point of view, it is worth to mention that glutamic anhydride **1** has been used as building block for the synthesis of glutamate-containing peptides when peptide chemistry was still in its infancy [22]. Compound **1** was subjected to ring opening with glycine *tert*-butyl ester, which resulted in quantitative consumption of the anhydride within 30 min under the formation of the regioisomeric  $\alpha$ - and  $\gamma$ -dipeptides **2** and **2a**. The ratio of both isomers was determined to be 7:3 in the favour to the desired product **2** by HPLC analysis (see Figure S1, Supporting Information). As reported by Leblanc *et al.*, both products were conveniently separated by chromatography on silica gel. By-product **2a** was characterised and could – in its  $N^{\alpha}$ -Fmoc-protected version – be a useful building block for solid-phase peptide synthesis as it represents an extended glutamate analogue. Dipeptide Z-Glu-Gly-O*t*Bu (**2**) was esterified with the fluorophore 4-methylumbelliferone by applying conditions that have been elaborated by Twibanire and Grindley for the efficient acylation of alcohols of varying reactivity using HATU as activating agent [23], which provided compound **3**. Column chromatographic purification of the crude product yielded the product, which contained an unknown impurity according to the  $^1\text{H}$  NMR spectrum beside trace amounts of unreacted 4-methylumbelliferone. As these impurities would be more difficult to remove after the final step considering the higher polarity



of the free carboxylic acid, the obtained material was recrystallised to furnish highly pure compound **3**. In the final step, *tert*-butyl ester **3** was cleaved by treatment with trifluoroacetic acid. During work-up, excessive TFA was efficiently removed by acidic aqueous washing to obtain the crude product in crystalline state. This material was recrystallised from ethyl acetate/acetonitrile/cyclohexane to obtain compound **4** as monohydrate, according to results of elementary microanalysis. Its purity has been confirmed by RP-HPLC/MS analysis.



**Scheme 1:** Four-step synthesis of Z-Glu(HMC)-Gly-OH (**4**) starting from Z-Glu-OH. Reagents and conditions: a) acetic anhydride, 55 °C, 10 min; b) H-Gly-OtBu·HCl, triethylamine, CHCl<sub>3</sub>, room temperature; c) HATU, DIPEA, 4-methylumbelliferone, DMF, room temperature; d) TFA, CH<sub>2</sub>Cl<sub>2</sub>, room temperature.

Compound **4** was investigated regarding the kinetics of hTGase 2-catalysed hydrolysis both at pH 6.5 and pH 8.0. The results are shown in Figure 1 and Table 1 (see also Figure S19 in Supporting Information). The obtained catalytic and Michaelis constants are in good agreement with the recently published values [14]. The fact that the determined  $K_m$  values are slightly lower than those recently published can be attributed to the better-defined composition of the crystalline compound material obtained herein whereas previously obtained substrate preparations furnished amorphous and slightly hygroscopic material after lyophilisation.

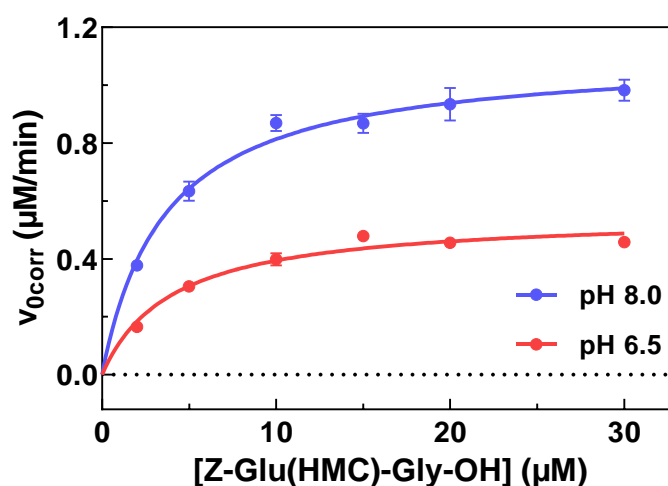


**Figure 1:** hTGase 2-catalysed hydrolysis of Z-Glu(HMC)-Gly-OH (**4**) at pH=8.0 and pH 6.5. Plots of  $v_{0\text{corr}}=f([4])$  for pH 8.0 and pH 6.5 with the nonlinear regressions (—) using Equation (3) (Michaelis-Menten equation, Materials and Methods section). Data shown are mean values  $\pm$ SEM of 3 separate experiments, each performed in duplicate. When not apparent, error bars are smaller than the symbols. Conditions: pH=8.0 or 6.5, 30 °C, 5% DMSO, 500  $\mu$ M TCEP, 3  $\mu$ g/ml of hTGase 2.

**Table 1:** Kinetic parameters for the hTGase 2-catalysed hydrolyses of Z-Glu(HMC)-Gly-OH (**4**) at pH 6.5 and 8.0

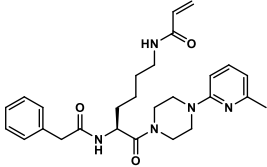
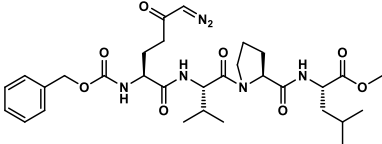
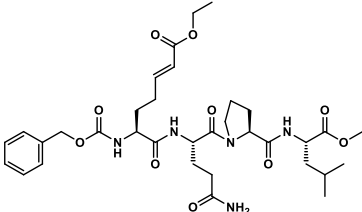
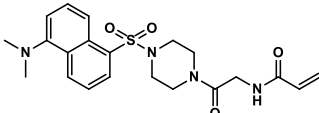
pH value	$K_m$ ( $\mu\text{M}$ )	$k_{\text{cat}}$ ( $\text{s}^{-1}$ )	$k_{\text{cat}}/K_m$ ( $\text{M}^{-1}\text{s}^{-1}$ )
6.5	4.05 (0.23)	0.30 (0.01)	74,100
8.0	3.93 (0.48)	0.61 (0.03)	155,000

Rate constant for spontaneous hydrolysis:  $k_{\text{obs}}$  (TCEP, pH 8.0) =  $16.8 (0.5) \times 10^{-3} \text{ min}^{-1}$

For details on calculation of the kinetic parameters see Materials and Methods Section. Data shown are mean values ( $\pm$ SEM) of three separate experiments, each performed in duplicate. Active concentrations of hTGase 2 ( $E_T=30.8 \text{ nM}$ ) were determined by active site titration as recently described [24].

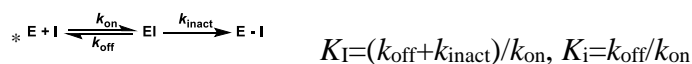
Following the hTGase 2-catalysed hydrolysis at pH 6.5, the utility of substrate **4** for the kinetic characterisation of irreversible inhibitors was demonstrated/validated by investigating three inhibitors which were reported in the literature. The selected compounds comprised the commercially available peptidic inhibitors Z006 and Z013, which bear a diazomethyl ketone or an  $\alpha,\beta$ -unsaturated carboxylic ester as electrophilic warhead, respectively. Furthermore, the nonpeptidic acrylamide 1-155 (compound **7**), which was recently published by Badarau et al. [21, 25], was synthesised according to Scheme 2 in orientation to the described procedure. In contrast to the former two compounds, a second-order inactivation constant  $k_{\text{inact}}/K_i$  has been reported for the latter. The results of the inhibitor characterisation are included in Table 2.

**Table 2:** Second-order inactivation constants ( $k_{\text{inact}}/K_i$ ) and  $K_i$  values of different literature-known irreversible inhibitors of hTGase 2 at pH 6.5 compared to their reported inhibitory parameters

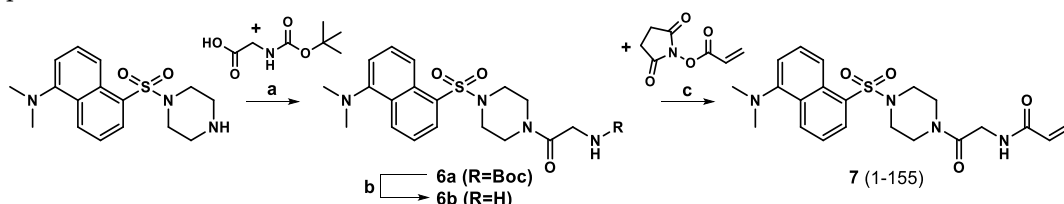
compound	structure	$k_{\text{inact}}/K_i$ ( $\text{M}^{-1}\text{s}^{-1}$ ) <sup>a*</sup>	$K_i$ ( $\mu\text{M}$ ) <sup>a*</sup>	$\text{IC}_{50}$ (nM)
<b>5</b>		4,880 (20) <sup>[15]</sup>	5.73 (0.77) <sup>[15]</sup>	310 <sup>[15]b</sup> 14 (8.2) <sup>[26]c</sup>
Z006		191,000 (3,000)	0.096 (0.01)	20 <sup>[27]c</sup>
Z013		51,500 (5,800)	0.45 (0.02)	200 <sup>[28]d</sup>
1-155 ( <b>7</b> )		12,700 (700) 4,962 <sup>[21]f</sup>	1.43 (0.01)	6.1 (0.4) <sup>[21]e</sup>

<sup>a</sup>Data shown are mean values ( $\pm$ SEM) of two separate experiments, each performed in duplicate.

<sup>b</sup>TGase 2-catalysed incorporation of R-I-Cad in DMC (transamidation) at pH 8.0 (5 min preincubation period of enzyme and inhibitor). <sup>c</sup>TGase 2-catalysed incorporation of Boc-K-NH(CH<sub>2</sub>)<sub>2</sub>NH-Dns in DMC (transamidation) at pH 7.4 (30 min preincubation period of enzyme and inhibitor). <sup>d</sup>Isopeptidase-assay using the substrate Abz-NE(CAD-DNP)EQVSPLTLTK-OH (A101, Zedira). <sup>e</sup>TGase 2-catalysed incorporation of *N*-(biotinyl)cadaverine in immobilised DMC (transamidation) at pH 8.5 (30 min preincubation period of enzyme and inhibitor). <sup>f</sup>GDH-coupled assay (deamidation) at pH 7.2.



Schaertl *et al.* have determined an IC<sub>50</sub> value of 20 nM for Z006 together with various other compounds by employing a fluorescence-based transamidase-detecting assay using *N,N*-dimethylcasein as acyl donor and *N*-monodansylcadaverin as acyl acceptor substrate, respectively [27]. In a later study, *N*<sup>ε</sup>-acryloyllysine-based irreversible inhibitor **5** has been synthesised, which was investigated in the same assay [26]. The IC<sub>50</sub> value of **5** was 14 nM under these conditions, which suggests that it should be equipotent to Z006. However, the *k*<sub>inact</sub>/*K*<sub>I</sub> value of Z006 determined herein (191 000 M<sup>-1</sup>s<sup>-1</sup>) is 37-fold greater than that of **5**. Even though the applied assay methods detect different TGase 2-catalysed reactions (transamidation in Schaertl *et al.* *vs.* hydrolysis herein) and the pH values are different (6.5 *vs.* 7.4), the potencies of Z006 and **5** should not be influenced to such extent. In agreement with the value of *k*<sub>inact</sub>/*K*<sub>I</sub> determined for Z006, Khosla's group reported inactivation constants of 48 000 M<sup>-1</sup>s<sup>-1</sup> [29] and 139 000 M<sup>-1</sup>s<sup>-1</sup> [30] for structurally related peptidic diazomethyl ketones, which have been determined using the GDH-coupled assay. The higher reactivity of Z006 towards TGase 2 in comparison to **5** is reasonable, as diazomethyl ketones are inherently more reactive towards thiols than acrylamides. Moreover, as the peptidic structures of Z006 and Z013 are based on gliadin peptides, which are natural substrates of TGase 2, they can probably be better accommodated by the active site, which in turn results in stronger non-covalent interactions. This is reflected in the low *K*<sub>I</sub> value of 96 nM for Z006. The similar IC<sub>50</sub> values of Z006 and **5** and the drastically differing inactivation constants can be rationalised when the assay conditions are considered. The IC<sub>50</sub> values were determined using a TGase 2 concentration of 20 nM and a preincubation time of 30 min [27]. Therefore, the IC<sub>50</sub> limit, which corresponds to half of the employed active enzyme concentration ([E]<sub>T</sub>/2) [31, 32], might have been reached for both compounds. In this context, it should be pointed out that the IC<sub>50</sub> value of an irreversible inhibitor in general will always be equal to [E]<sub>T</sub>/2, provided that [inhibitor] ≥ [enzyme]/2 and enough incubation time is given. The other investigated peptidic inhibitor Z013 exhibits a *k*<sub>inact</sub>/*K*<sub>I</sub> of 51 500 M<sup>-1</sup>s<sup>-1</sup>, which is significantly more potent than **5**. As for Z006, the higher inhibitory potency of Z013 can be attributed to the more reactive electrophilic warhead and the peptidic structure, which corresponds to that of Z006, apart from one amino acid side chain. An IC<sub>50</sub> value of 200 nM has been reported for Z013; however, no information on enzyme concentration and preincubation time were provided [28]. Again, the comparison to the kinetic parameter *k*<sub>inact</sub>/*K*<sub>I</sub> indicates that IC<sub>50</sub> values are not suitable for evaluating the potency of irreversible inhibitors, unless identical conditions and carefully adjusted preincubation times are used [33].



**Scheme 2: Synthesis of inhibitor 1-155**

Reagents and conditions: **a**) PyBOP, DIPEA, DMF, 3 h; **b**) TFA/CH<sub>2</sub>Cl<sub>2</sub> (1:1, v/v), 2 h; **c**) TEA, CH<sub>2</sub>Cl<sub>2</sub>, 2 h.

The synthesis of 1-155 (compound **7**) started with the amide bond coupling between Boc-Gly-OH and *N*-monodansylpiperazine to **6a** using PyBOP and DIPEA, in difference to the published procedure, which used EDC, HOBt and NMM as coupling reagents (Scheme 2) [21]. After TFA-

mediated Boc cleavage the acryloyl moiety was introduced by reacting **6b** with *N*-acryloxysuccinimide. The last step proceeded in low yield and should better be performed with acryloyl chloride as acylating agent. A  $k_{\text{inact}}/K_{\text{I}}$  of  $12\,700\,\text{M}^{-1}\text{s}^{-1}$  was determined for 1-155. This value is approximately 2.5-fold higher than both that for the *N* $^{\epsilon}$ -acryloyllysine **5** and that of 1-155 determined by Badarau *et al.* using the GDH-coupled assay. However, taking into account that the two assay methods work at different pH values (6.5 *vs.* 7.2) the results can be considered comparable. The higher efficiency of 1-155 compared to **5** as determined in the fluorimetric assay is remarkable. This is probably the result of well-balanced conformational flexibility/rigidity and targeting of interaction partners in the enzymes binding site for 1-155. Considering its smaller size (30 *vs.* 35 non-hydrogen atoms), binding of 1-155 might be entropically more favoured than that of **5**.

In addition to the kinetic characterisation of inhibitors, a further asset of the fluorogenic substrate **4** is the convenient investigation of amine-based acyl acceptor substrates, which are interesting for the development of TGase 2-directed imaging agents [34]. Moreover, their substrate properties are of general interest. Therefore, we decided to determine exemplarily the kinetic parameters of histamine, serotonin and dopamine as common biogenic amines of the primary arylethylamine type. These compounds are known as classical neurotransmitters and the former two are important mediators in non-neuronal cells and tissues as well. They have been known for 60 years to be substrates of TGase 2 [35]. However, the physiological significance of TGase-mediated aminylation as an important post-translational modification has been recognised only in the recent decades [36–39]. In particular, the TGase 2-catalysed serotonylation of small GTPases such as RhoA and Rab4 in thrombocytes has been shown to be critical for blood haemostasis. Worth of note, serotonylation of Gln63 in RhoA renders its GTPase activity permanently active [40]. A similar mechanism has been identified for the constitutive activation of Rac1 in the central nervous system [41, 42]. In particular, activation of the  $G_{q/11}$ -coupled 5-HT<sub>2A</sub> receptors in rat cortical cells raises the cytosolic  $\text{Ca}^{2+}$  level, which in turn activates TGase 2 for catalysing the serotonylation of Rac1 [42]. Apart from small GTPases, other proteins have been identified as substrates for TGase 2-mediated serotonylation [43] and, most recently, the transamidation of Gln5 of histone H3 to serotonin has been discovered as a transcription-permissive modification [44]. Similar to serotonylation, TGase 2-mediated histaminylation leads to the constitutive activation of small and heterotrimeric G proteins [45]. Histamine transfer to extracellular proteins such as fibrinogen has been suggested as a mechanism for attenuating the pro-inflammatory effects of this endogenous mediator [46]. Furthermore, fibronectin, another extracellular TGase 2 substrate, has been shown to undergo monoaminylation, including dopaminylation [47, 48]. Despite this overwhelming body of evidence for the biological relevance of TGase 2-catalysed protein acyl transfer to biogenic monoamines, exact kinetic data on their substrate properties are scarce or have not been determined at all.

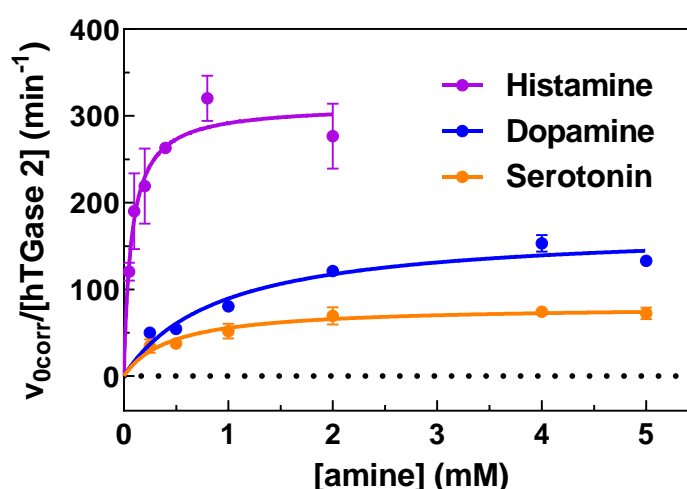


**Figure 2.** hTGase 2-catalysed incorporation of different biogenic amines into compound Z-Glu(HMC)-Gly-OH (4). Plots of  $v_{0\text{corr}}/[\text{hTGase 2}] = f([\text{amine}])$  with nonlinear regressions (—) using Equation (3) (Michaelis-Menten equation, Materials and Methods section). Data shown are mean values  $\pm$ SEM of two separate experiments, each performed in duplicate. When not apparent, error bars are smaller than the symbols. Conditions: pH=8.0 (100 mM MOPS was used, which ensures that the pH value is maintained over the entire range of amine concentrations), 30 °C, 5% DMSO, 100  $\mu$ M Z-Glu(HMC)-Gly-OH (4), 500  $\mu$ M TCEP, 0.6, 2 and 3  $\mu$ g/mL of hTGase 2 for histamine, dopamine and serotonin, respectively.

**Table 3.** Kinetic parameters of different biogenic amines as acyl acceptors for hTGase 2 at pH=8.0

biogenic amine	$K_m^{\text{app}}$ (mM)	$k_{\text{cat}}^{\text{app}}$ ( $\text{s}^{-1}$ )	$k_{\text{cat}}/K_m$ ( $\text{M}^{-1}\text{s}^{-1}$ )
histamine	0.08 (0.01)	5.35 (0.58)	66,900
dopamine	0.96 (0.06)	2.90 (0.04)	3,000
serotonin	0.50 (0.17)	1.35 (0.04)	2,700

For details on calculation of the kinetic parameters see Experimental section. Data shown are mean values ( $\pm$ SEM) of two separate experiments, each performed in duplicate. Active concentrations of hTGase 2 ( $E_T=6.15$  nM for histamine, 20.5 nM for dopamine and 30.8 nM for serotonin) were determined by active site titration as recently described [24].

The results on the kinetic characterisation of histamine, serotonin and dopamine are shown in Figure 2 and the calculated parameters are included in Table 3 (see also Figure S20 in Supporting Information). The substrate concentration range and the employed enzyme concentration were adjusted for each substrate in preliminary tests. Notably, no substrate inhibition occurred for any of the amine substrates. The formation of the corresponding secondary amide products upon TGase 2-catalysed substrate conversion was confirmed by LC-MS/MS analysis (see Figures S21-S26 in Supporting Information). In agreement with previously published data using the GDH-coupled assay and the gluten-derived heptapeptide Ac-PQPQLPF-NH<sub>2</sub> as acyl donor, histamine is a very efficient acyl acceptor substrate for TGase 2 [49]. In contrast, the second-order performance constants for both serotonin and dopamine are approximately 20-fold lower. In the GDH-assay mentioned before, which employs TGase 2 at a concentration as high as 50  $\mu$ g/mL (640 nM), conversion of serotonin was not detectable. This enzyme concentration is approximately 20-fold higher than that applied herein for the analysis of serotonin. This demonstrates the value of activated fluorogenic acyl donors such as compound 4 as even poor acyl acceptor substrates can be analysed and the consumption of valuable enzyme material is minimised. According to its  $k_{\text{cat}}/K_m$ , dopamine is a slightly more efficient amine substrate for TGase 2 than serotonin, even though the apparent Michaelis constant is lower for serotonin. Considering that all three studied biogenic amines share the 2-aminoethyl chain and an (hetero)aromatic core, the distinct substrate properties of histamine are remarkable. One could argue that its imidazole ring could assist in the deacylation step of the catalytic cycle by acting as general base in the proton transfer from the amine nitrogen, as intramolecular hydrogen bonds have been identified in both the neutral and side-chain protonated form of histamine [50]. Thus, the imidazole ring of the substrate would fulfil the same function during attack of the neutral amino group on the thioester intermediate as the imidazole of active-site His335 [51]. However, its  $K_m^{\text{app}}$  of 80  $\mu$ M, which is significantly lower than the corresponding values for dopamine and serotonin, suggests specific interactions within the enzyme's active site. Furthermore, it is surprising that serotonin is the least efficient substrate of the investigated amines even though the most findings on physiologically relevant protein monoaminylation have been obtained for this biogenic amine [52]. In this context, it is worth to consider that beside availability of the particular monoamine substrate, which can vary from cell type and depends on the subcellular localisation, the

sequence in which the Gln substrate residue is embedded should also influence the substrate specificity towards the amine-based acyl acceptor substrate. This is evidenced by investigations on the sequence dependence of TGase 2-catalysed modification of Hsp20, which occurs at two of its five Gln residues, Gln31 and Gln66. Interestingly, concerning the differentiation between the acyl acceptor the outcome is different for both residues as Gln31 is exclusively transamidated whereas Gln66 is exclusively deamidated. However, when the isolated undecapeptides of the sequences in which both residues are embedded are considered, Gln31 is not converted at all whereas Gln66 undergoes both transamidation and deamidation [53]. This indicates that the results on the substrate properties of the biogenic monoamines obtained with Z-Glu(HMC)-Gly-OH (**4**) as acyl donor substrate should be extrapolated with care towards large protein substrates. Therefore, we would like to define the elucidation of the molecular mechanisms that lead to the coupling between acyl donor and acyl acceptor substrate specificity as a future challenge for TGase research. In this context, the influence of the acceptor nucleophile on the mechanism of the acylation step in TGase 2 catalysis has been established very recently on the basis of  $^{14}\text{N}/^{15}\text{N}$  kinetic isotope effects [54].

#### 4. Conclusions

A reliable solution phase synthesis of the title substrate compound **4** has been established, which will support its use in transglutaminase research. Its value for the evaluation of TGase 2 inhibitors based on meaningful kinetic parameters has been demonstrated. The compound's utility for the characterisation of amine substrates as exemplified by the biogenic amines histamine, serotonin and dopamine has been shown, which allows for the first time their comparison on a robust kinetic basis.

**Supporting Information:** Supplementary data associated with this article (chromatograms for synthesis, NMR spectra for compounds **1-4**, kinetic data, identification of reaction products for biogenic amines) can be found in the online version at doi:

**Acknowledgments:** We highly appreciate the skilful assistance of Ms. Peggy Nehring and Mr. Kay Fischer in substrate synthesis and that of Mr. David Bauer in that of inhibitor **1-155**. Dr. Markus Laube and Ms. Karin Landrock are kindly acknowledged for the measurement of HR-MS spectra and elemental microanalyses, respectively.

#### References

- [1] N. Agnihotri, K. Mehta, Transglutaminase-2: Evolution from pedestrian protein to a promising therapeutic target, *Amino Acids*, 49 (2017) 425-439.
- [2] R.L. Eckert, Transglutaminase 2 takes center stage as a cancer cell survival factor and therapy target, *Mol. Carcinog.*, 58 (2019) 837-853.
- [3] J.E. Folk, J.S. Finlayson, The  $\epsilon$ -( $\gamma$ -glutamyl)lysine crosslink and the catalytic role of transglutaminases, *Adv. Protein Chem.*, 31 (1977) 1-133.
- [4] R. van Geel, M.F. Debets, D.W. Lowik, G.J. Pruijn, W.C. Boelens, Detection of transglutaminase activity using click chemistry, *Amino Acids*, 43 (2012) 1251-1263.
- [5] S. Hauser, R. Wodtke, C. Tondera, J. Wodtke, A.T. Neffe, J. Hampe, A. Lendlein, R. Löser, J. Pietzsch, Characterization of tissue transglutaminase as a potential biomarker for tissue response toward biomaterials, *ACS Biomater. Sci. Eng.*, 5 (2019) 5979-5989.
- [6] K. Jambrovics, I.P. Uray, Z. Keresztessy, J.W. Keillor, L. Fesus, Z. Balajthy, Transglutaminase 2 programs differentiating acute promyelocytic leukemia cells in all-trans retinoic acid treatment to inflammatory stage through NF- $\kappa$ B activation, *Haematologica*, 104 (2019) 505-515.

- [7] M.S. Pavlyukov, N.V. Antipova, M.V. Balashova, M.I. Shakhparonov, Detection of transglutaminase 2 conformational changes in living cell, *Biochem. Biophys. Res. Commun.*, 421 (2012) 773-779.
- [8] N.S. Caron, L.N. Munsie, J.W. Keillor, R. Truant, Using FLIM-FRET to measure conformational changes of transglutaminase type 2 in live cells, *PLoS One*, 7 (2012) e44159.
- [9] S. Liu, R.A. Cerione, J. Clardy, Structural basis for the guanine nucleotide-binding activity of tissue transglutaminase and its regulation of transamidation activity, *Proc. Natl. Acad. Sci. USA*, 99 (2002) 2743-2747.
- [10] W.P. Katt, M.A. Antonyak, R.A. Cerione, Opening up about tissue transglutaminase: When conformation matters more than enzymatic activity, *Med One*, 3 (2018).
- [11] A. Case, R.L. Stein, Kinetic analysis of the interaction of tissue transglutaminase with a nonpeptidic slow-binding inhibitor, *Biochemistry*, 46 (2007) 1106-1115.
- [12] K. Thangaraju, B. Biri, G. Schlosser, B. Kiss, L. Nyitray, L. Fesus, R. Kiraly, Real-time kinetic method to monitor isopeptidase activity of transglutaminase 2 on protein substrate, *Anal. Biochem.*, 505 (2016) 36-42.
- [13] M. Pietsch, R. Wodtke, J. Pietzsch, R. Löser, Tissue transglutaminase: An emerging target for therapy and imaging, *Bioorg. Med. Chem. Lett.*, 23 (2013) 6528-6543.
- [14] R. Wodtke, G. Schramm, J. Pietzsch, M. Pietsch, R. Löser, Synthesis and kinetic characterisation of water-soluble fluorogenic acyl donors for transglutaminase 2, *ChemBioChem*, 17 (2016) 1263-1281.
- [15] R. Wodtke, C. Hauser, G. Ruiz-Gómez, E. Jäckel, D. Bauer, M. Lohse, A. Wong, J. Pufe, F.-A. Ludwig, S. Fischer, S. Hauser, D. Greif, M.T. Pisabarro, J. Pietzsch, M. Pietsch, R. Löser, *N*<sup>ε</sup>-Acryloyllysine piperazides as irreversible inhibitors of transglutaminase 2: Synthesis, structure-activity relationships, and pharmacokinetic profiling, *J. Med. Chem.*, 61 (2018) 4528-4560.
- [16] S.I. Chung, R.I. Shrager, J.E. Folk, Mechanism of action of guinea pig liver transglutaminase. VII. Chemical and stereochemical aspects of substrate binding and catalysis, *J. Biol. Chem.*, 245 (1970) 6424-6435.
- [17] A. Leblanc, C. Gravel, J. Labelle, J.W. Keillor, Kinetic studies of guinea pig liver transglutaminase reveal a general-base-catalyzed deacylation mechanism, *Biochemistry*, 40 (2001) 8335-8342.
- [18] N.J. Manesis, M. Goodman, Synthesis of a novel class of peptides: Dilactam-bridged tetrapeptides, *J. Org. Chem.*, 52 (1987) 5331-5341.
- [19] D.S. Pedersen, Let's talk about TLCs. Part 2 - hanessian's stain, 2006. <http://curlyarrow.blogspot.com/2006/11/lets-talk-about-tlcs-part-2-hanessians.html>; accessed on 10/12/2019.
- [20] E. Klieger, E. Schröder, Synthese von  $\alpha$ -Glutamyl-Peptiden mit Carbobenzoxy-L-glutaminsäure- $\alpha$ -phenylester, *Liebigs Ann. Chem.*, 661 (1963) 193-201.
- [21] E. Badarau, Z. Wang, D.L. Rathbone, A. Costanzi, T. Thibault, C.E. Murdoch, S. El Alaoui, M. Bartkeviciute, M. Griffin, Development of potent and selective tissue transglutaminase inhibitors: Their effect on TG2 function and application in pathological conditions, *Chem. Biol.*, 22 (2015) 1347-1361.
- [22] M. Bergmann, L. Zervas, Über ein allgemeines Verfahren der Peptid-Synthese, *Ber. Dtsch. Chem. Ges.*, 65 (1932) 1192-1201.
- [23] J.D. Twibanire, T.B. Grindley, Efficient and controllably selective preparation of esters using uronium-based coupling agents, *Org. Lett.*, 13 (2011) 2988-2991.
- [24] C. Hauser, R. Wodtke, R. Löser, M. Pietsch, A fluorescence anisotropy-based assay for determining the activity of tissue transglutaminase, *Amino Acids*, 49 (2017) 567-583.
- [25] M. Griffin, D. Rathbone, B.L. Eduard, Acylpiperazines as inhibitors of transglutaminase and their use in medicine. WIPO Patent WO 2014/057266 A1, April 17, 2014.
- [26] J. Wityak, M.E. Prime, F.A. Brookfield, S.M. Courtney, S. Erfan, S. Johnsen, P.D. Johnson, M. Li, R.W. Marston, L. Reed, D. Vaidya, S. Schaertl, A. Pedret-Dunn, M. Beconi, D. Macdonald, I. Muñoz-Sanjuan, C.



- Dominguez, SAR development of lysine-based irreversible inhibitors of transglutaminase 2 for huntington's disease, *ACS Med. Chem. Lett.*, 3 (2012) 1024-1028.
- [27] S. Schaertl, M. Prime, J. Wityak, C. Dominguez, I. Muñoz-Sanjuan, R.E. Pacifici, S. Courtney, A. Scheel, D. Macdonald, A profiling platform for the characterization of transglutaminase 2 (TG2) inhibitors, *J. Biomol. Screen.*, 15 (2010) 478-487.
- [28] Zedira - Z-MA-QPL-OMe, [https://zedira.com/Mechanism-of-TG-inhibitors/Michael-acceptor-peptidomimetics/Z-MA-QPL-OMe\\_Z013](https://zedira.com/Mechanism-of-TG-inhibitors/Michael-acceptor-peptidomimetics/Z-MA-QPL-OMe_Z013); accessed on 10/12/2019.
- [29] F. Hausch, T. Halttunen, M. Mäki, C. Khosla, Design, synthesis, and evaluation of gluten peptide analogs as selective inhibitors of human tissue transglutaminase, *Chem. Biol.*, 10 (2003) 225-231.
- [30] D.M. Pinkas, P. Strop, A.T. Brunger, C. Khosla, Transglutaminase 2 undergoes a large conformational change upon activation, *PLoS Biol.*, 5 (2007) e327.
- [31] J.W. Williams, J.F. Morrison, The kinetics of reversible tight-binding inhibition, *Methods Enzymol.*, 63 (1979) 437-467.
- [32] P.F. Cook, W.W. Cleland, *Enzyme kinetics and mechanism*, Garland Science Publishing, London, New York, 2007, p. 203.
- [33] R.A. Copeland, *Evaluation of enzyme inhibitors in drug discovery*, 2<sup>nd</sup> ed., John Wiley & Sons, Hoboken, NJ, 2013, p. 350.
- [34] B. van der Wildt, A.A. Lammertsma, B. Drukarch, A.D. Windhorst, Strategies towards in vivo imaging of active transglutaminase type 2 using positron emission tomography, *Amino Acids*, 49 (2017) 585-595.
- [35] D.D. Clarke, M.J. Mycek, A. Neidle, H. Waelsch, The incorporation of amines into protein, *Arch. Biochem. Biophys.*, 79 (1959) 338-354.
- [36] D.J. Walther, S. Stahlberg, J. Vowinckel, Novel roles for biogenic monoamines: From monoamines in transglutaminase-mediated post-translational protein modification to monoaminylation deregulation diseases, *FEBS J.*, 278 (2011) 4740-4755.
- [37] N.A. Muma, Z. Mi, Serotonylation and transamidation of other monoamines, *ACS Chem. Neurosci.*, 6 (2015) 961-969.
- [38] T.S. Lai, C.J. Lin, C.S. Greenberg, Role of tissue transglutaminase-2 (TG2)-mediated aminylation in biological processes, *Amino Acids*, 49 (2017) 501-515.
- [39] N.A. Muma, Transglutaminase in receptor and neurotransmitter-regulated functions, *Med One*, 3 (2018).
- [40] D.J. Walther, J.-U. Peter, S. Winter, M. Hölte, N. Paulmann, M. Grohmann, J. Vowinckel, V. Alamo-Bethencourt, C.S. Wilhelm, G. Ahnert-Hilger, M. Bader, Serotonylation of small GTPases is a signal transduction pathway that triggers platelet  $\alpha$ -granule release, *Cell*, 115 (2003) 851-862.
- [41] Y. Dai, N.L. Dudek, T.B. Patel, N.A. Muma, Transglutaminase-catalyzed transamidation: A novel mechanism for Rac1 activation by 5-HT<sub>2a</sub> receptor stimulation, *J. Pharmacol. Exp Ther.*, 326 (2008) 153-162.
- [42] Y. Dai, N.L. Dudek, Q. Li, N.A. Muma, Phospholipase C, Ca<sup>2+</sup>, and calmodulin signaling are required for 5-HT<sub>2a</sub> receptor-mediated transamidation of Rac1 by transglutaminase, *Psychopharmacology (Berlin)*, 213 (2011) 403-412.
- [43] J.C. Lin, C.C. Chou, Z. Tu, L.F. Yeh, S.C. Wu, K.H. Khoo, C.H. Lin, Characterization of protein serotonylation via bioorthogonal labeling and enrichment, *J. Proteome Res.*, 13 (2014) 3523-3529.
- [44] L.A. Farrelly, R.E. Thompson, S. Zhao, A.E. Lepack, Y. Lyu, N.V. Bhanu, B. Zhang, Y.E. Loh, A. Ramakrishnan, K.C. Vadodaria, K.J. Heard, G. Erikson, T. Nakadai, R.M. Bastle, B.J. Lukasak, H. Zebroski, 3rd, N. Alenina, M. Bader, O. Berton, R.G. Roeder, H. Molina, F.H. Gage, L. Shen, B.A. Garcia, H. Li, T.W. Muir, I.



- Maze, Histone serotonylation is a permissive modification that enhances TFIID binding to H3K4me3, *Nature*, 567 (2019) 535-539.
- [45] J. Vowinckel, S. Stahlberg, N. Paulmann, K. Bluemlein, M. Grohmann, M. Ralser, D.J. Walther, Histaminylation of glutamine residues is a novel posttranslational modification implicated in G-protein signaling, *FEBS Lett.*, 586 (2012) 3819-3824.
- [46] T.S. Lai, C.S. Greenberg, Histaminylation of fibrinogen by tissue transglutaminase-2 (TGM-2): Potential role in modulating inflammation, *Amino Acids*, 45 (2013) 857-864.
- [47] R. Hummerich, J.O. Thumfart, P. Findeisen, D. Bartsch, P. Schloss, Transglutaminase-mediated transamidation of serotonin, dopamine and noradrenaline to fibronectin: Evidence for a general mechanism of monoaminylation, *FEBS Lett.*, 586 (2012) 3421-3428.
- [48] R. Hummerich, V. Costina, P. Findeisen, P. Schloss, Monoaminylation of fibrinogen and glia-derived proteins: Indication for similar mechanisms in posttranslational protein modification in blood and brain, *ACS Chem. Neurosci.*, 6 (2015) 1130-1136.
- [49] S.W. Qiao, J. Piper, G. Haraldsen, I. Oynebraten, B. Fleckenstein, O. Molberg, C. Khosla, L.M. Sollid, Tissue transglutaminase-mediated formation and cleavage of histamine-gliadin complexes: Biological effects and implications for celiac disease, *J. Immunol.*, 174 (2005) 1657-1663.
- [50] P.I. Nagy, Competing intramolecular vs. Intermolecular hydrogen bonds in solution, *Int. J. Mol. Sci.*, 15 (2014) 19562-19633.
- [51] J.W. Keillor, C.M. Clouthier, K.Y. Apperley, A. Akbar, A. Mulani, Acyl transfer mechanisms of tissue transglutaminase, *Bioorg. Chem.*, 57 (2014) 186-197.
- [52] M. Bader, Serotonylation: Serotonin signaling and epigenetics, *Front. Mol. Neurosci.*, 12 (2019) 288.
- [53] J. Stamnaes, B. Fleckenstein, L.M. Sollid, The propensity for deamidation and transamidation of peptides by transglutaminase 2 is dependent on substrate affinity and reaction conditions, *Biochim. Biophys. Acta*, 1784 (2008) 1804-1811.
- [54] E.A. Wells, M.A. Anderson, T.N. Zeczycki, (15)(V/K) kinetic isotope effect and steady-state kinetic analysis for the transglutaminase 2 catalyzed deamidation and transamidation reactions, *Arch. Biochem. Biophys.*, 643 (2018) 57-61.

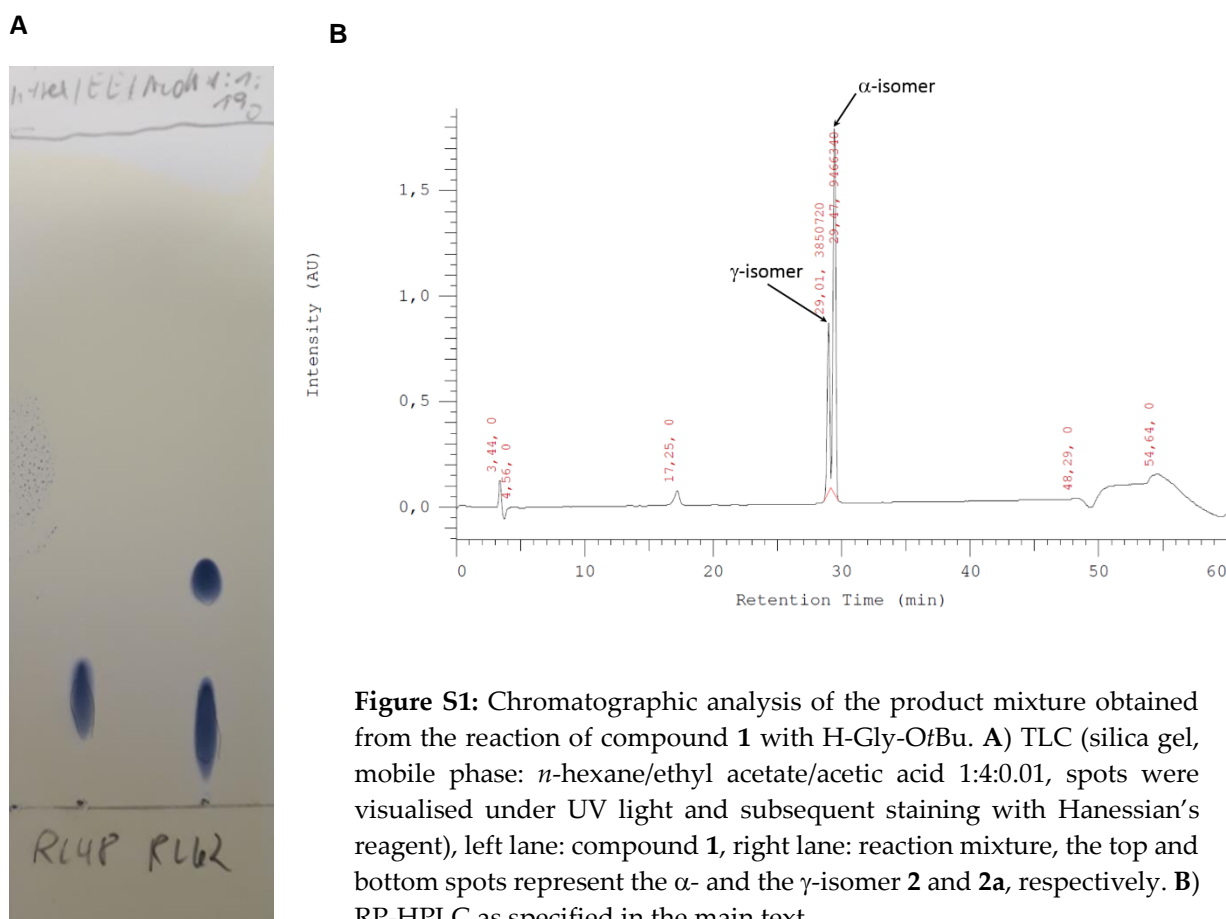
## Supporting Information

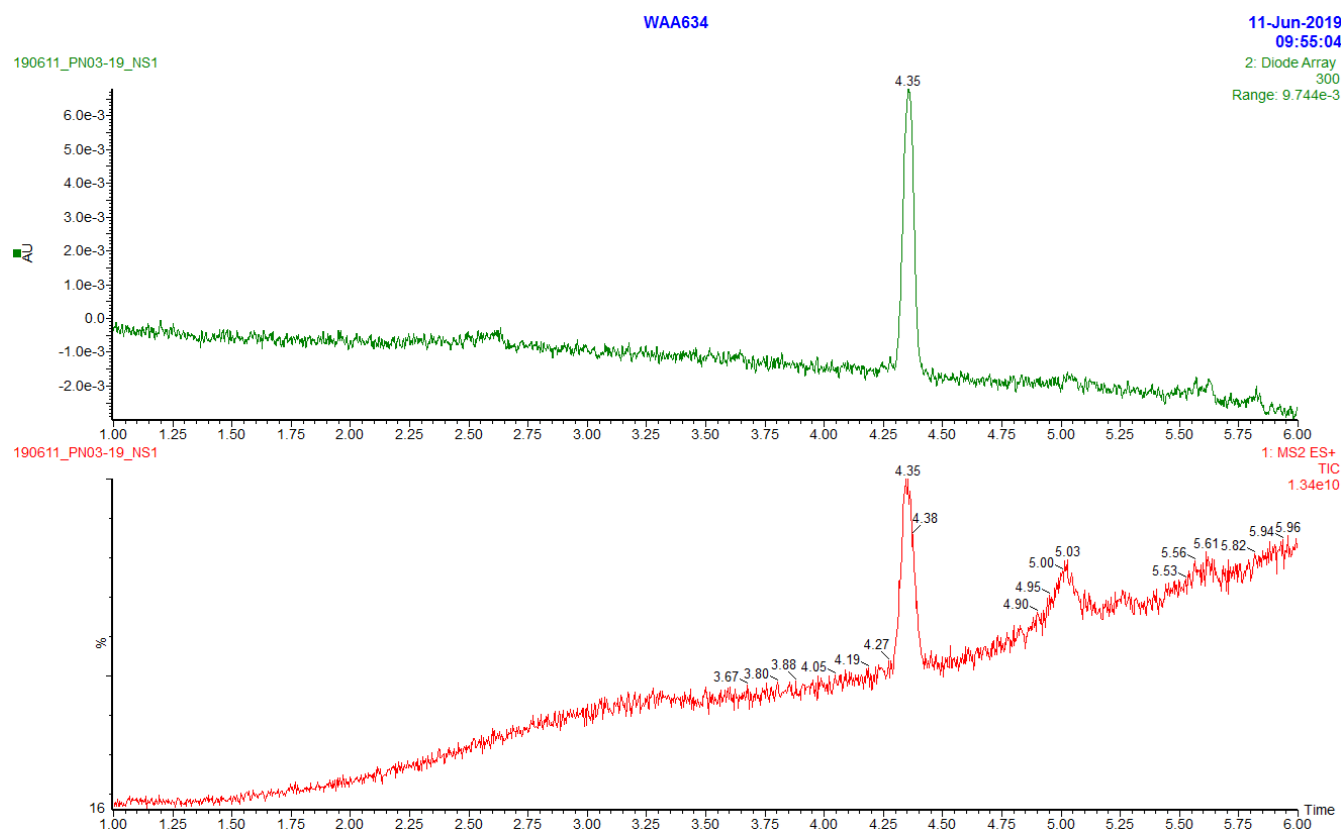
# Solution-Phase Synthesis of the Fluorogenic TGase 2 Acyl Donor Z-Glu(HMC)-Gly-OH and its Use for Inhibitor and Amine Substrate Characterisation

Robert Wodtke <sup>1\*</sup>, Markus Pietsch <sup>2</sup> and Reik Löser <sup>1,3\*</sup>

- 1 Helmholtz-Zentrum Dresden-Rossendorf, Institute of Radiopharmaceutical Cancer Research; Bautzner Landstrasse 400, 01328 Dresden, Germany
- 2 Institute II of Pharmacology, Centre of Pharmacology, Medical Faculty, University of Cologne, Gleueler Strasse 24, 50931 Cologne, Germany
- 3 Faculty of Chemistry and Food Chemistry, School of Science, Technische Universität Dresden, Mommsenstraße 4, 01062 Dresden, Germany

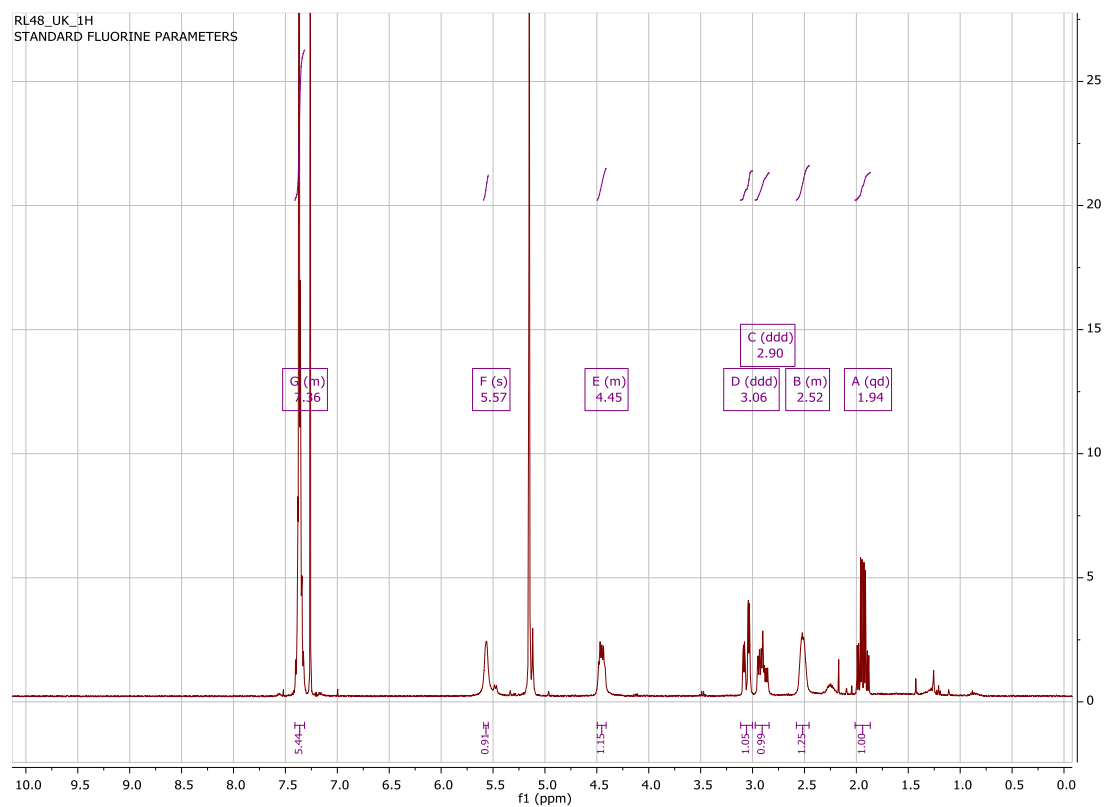
\*Email: r.wodtke@hzdr.de, r.loeser@hzdr.de



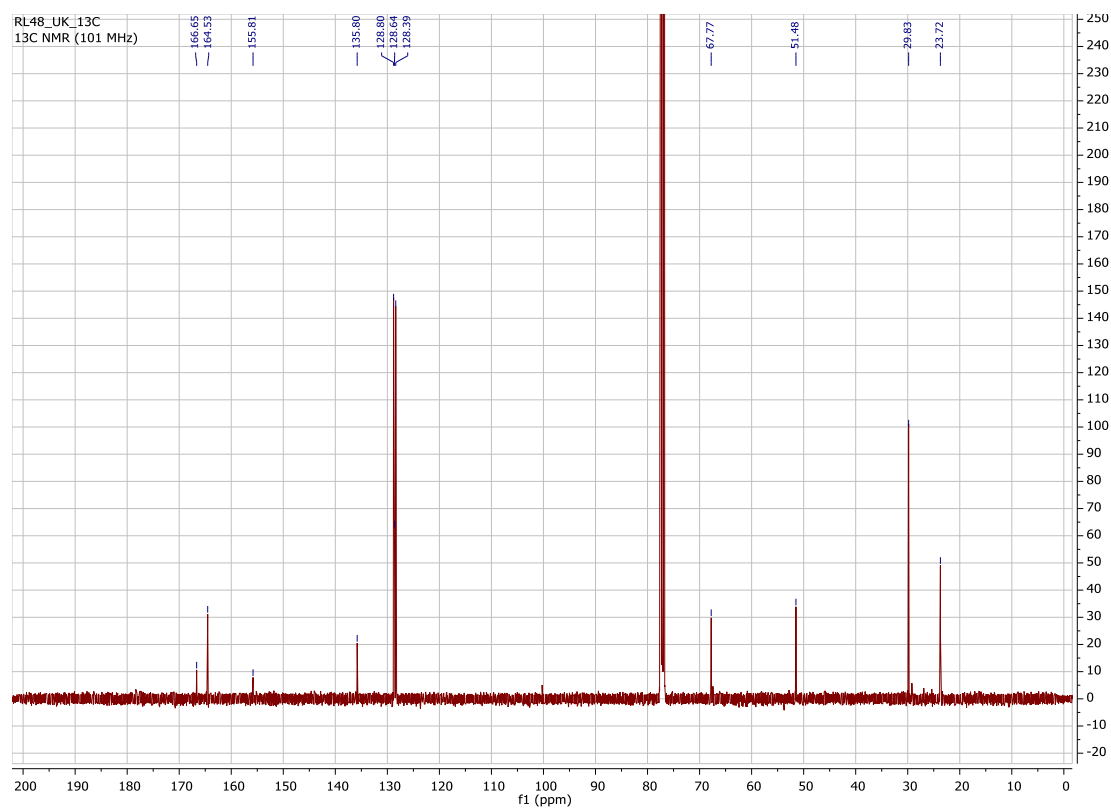


**Figure S2:** UPLC-MS analysis of Z-Glu(HMC)-Gly-OH (**4**). The upper panel shows the UV trace at 300 nm of the photo diode array (PDA) detector. The lower panel shows the total ion current as detected by the ESI-MS detector. For details of UPLC-MS analysis see Scheme S1.

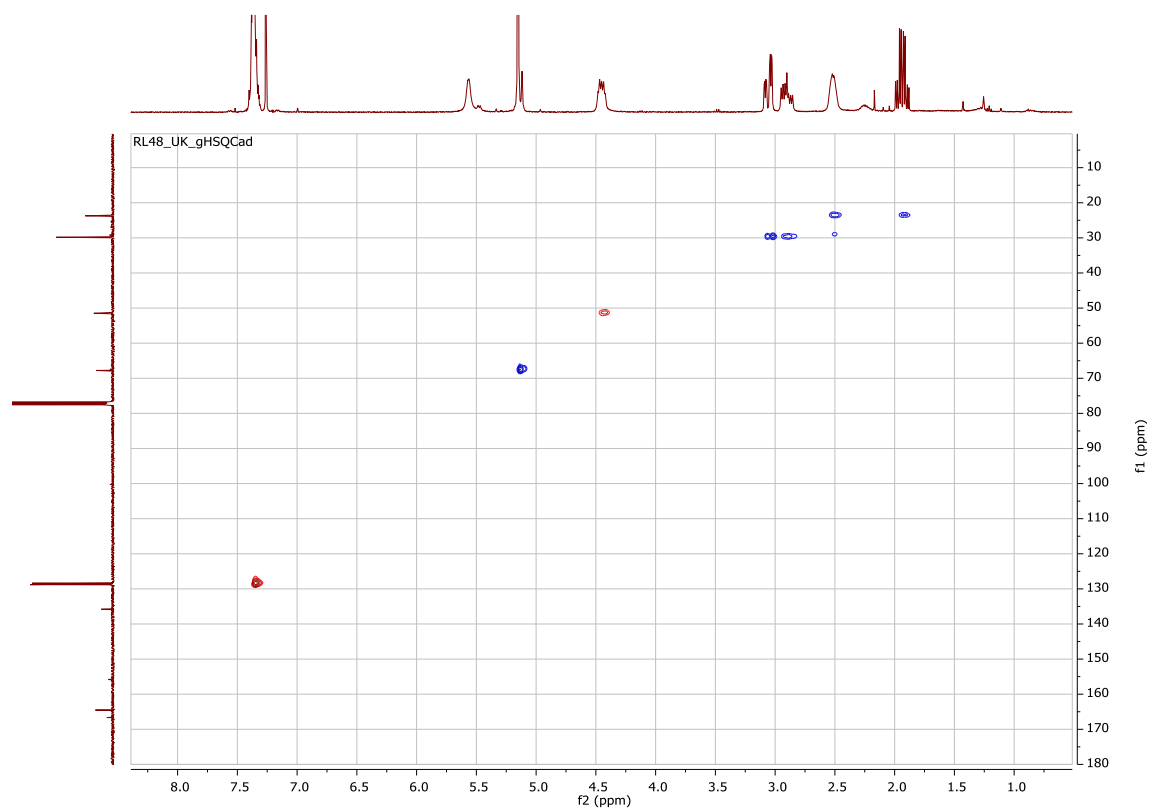
**Figure S3:**  $^1\text{H}$  NMR Spectrum of compound **1**



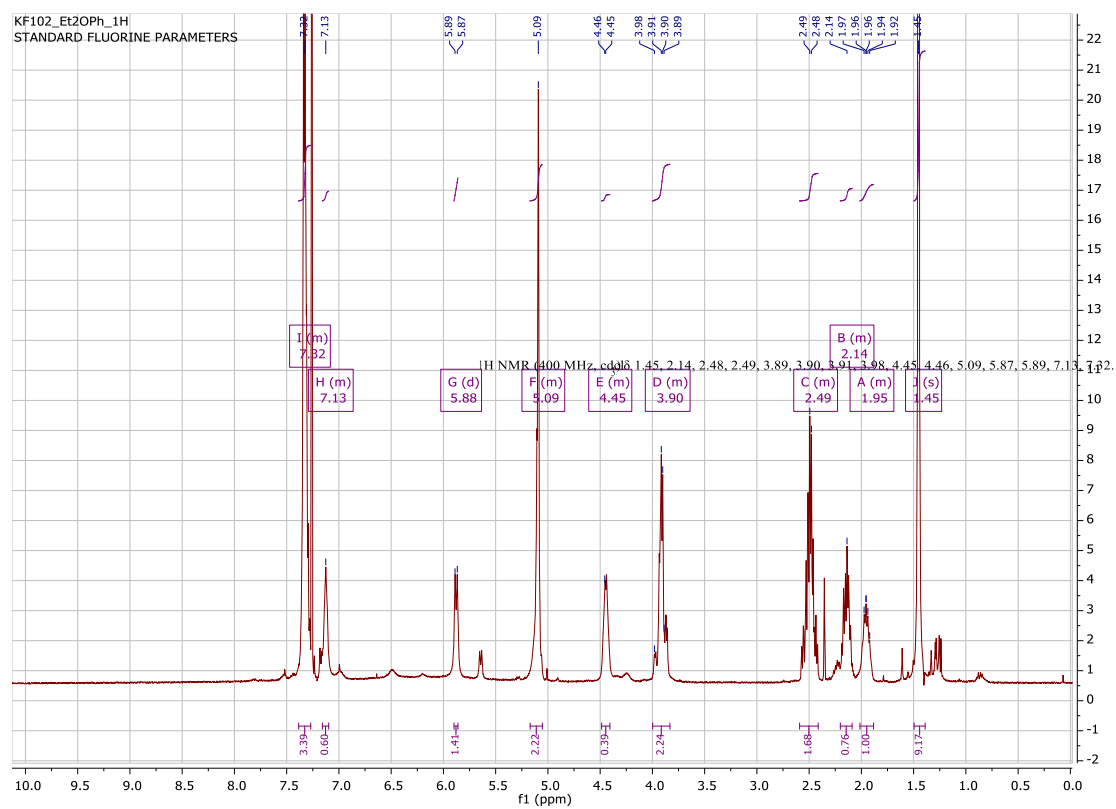
**Figure S4:**  $^{13}\text{C}$  NMR Spectrum of compound **1**



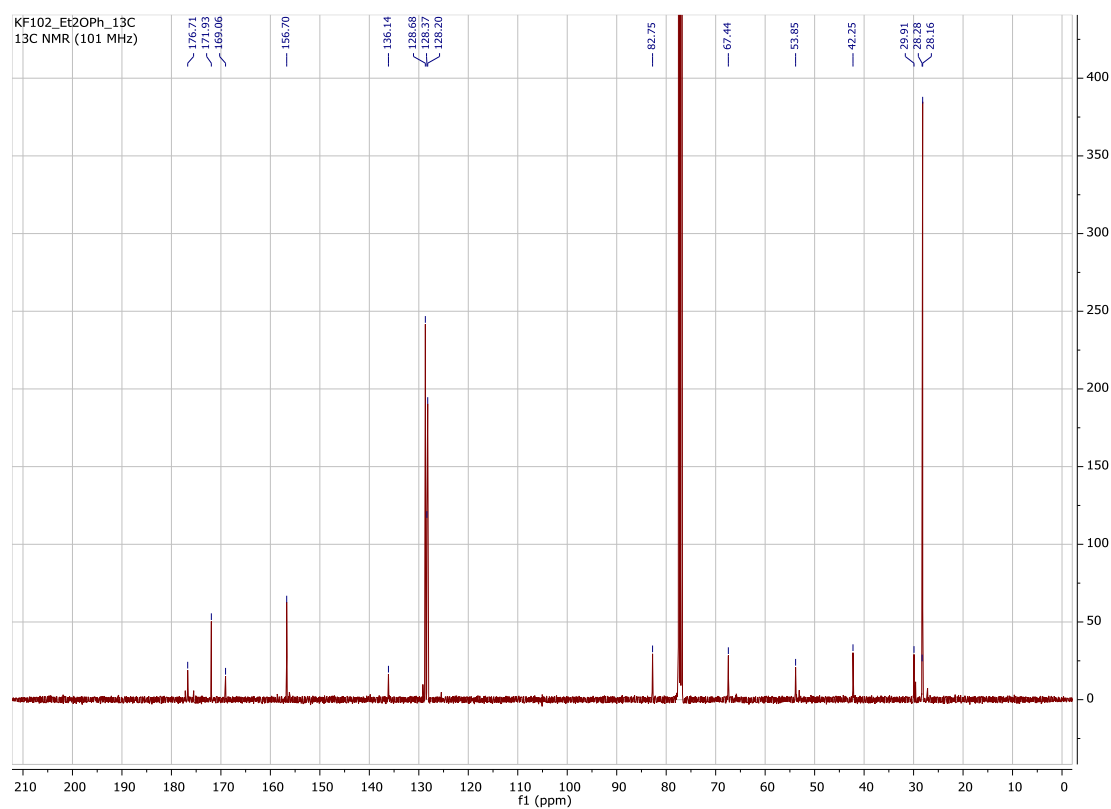
**Figure S5:**  $^1\text{H}$ ,  $^{13}\text{C}$  HSQC Spectrum of compound **1**



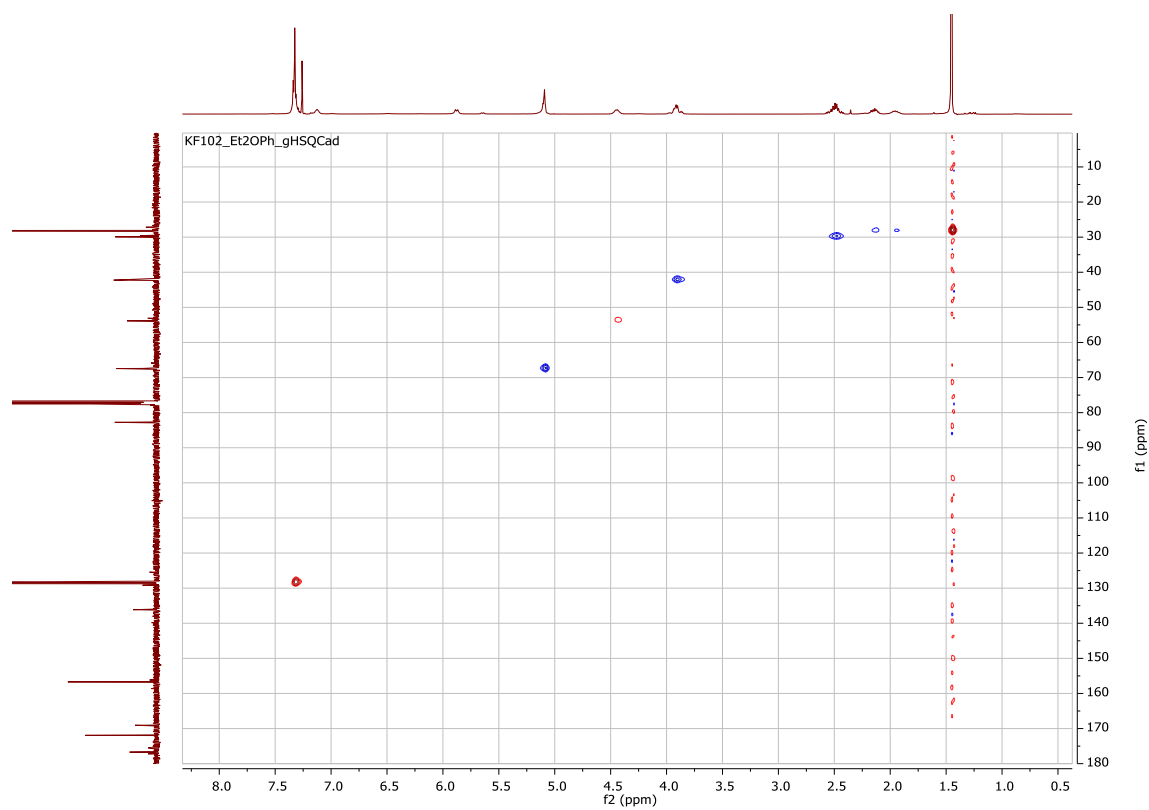
**Figure S6:**  $^1\text{H}$  NMR Spectrum of compound **2**



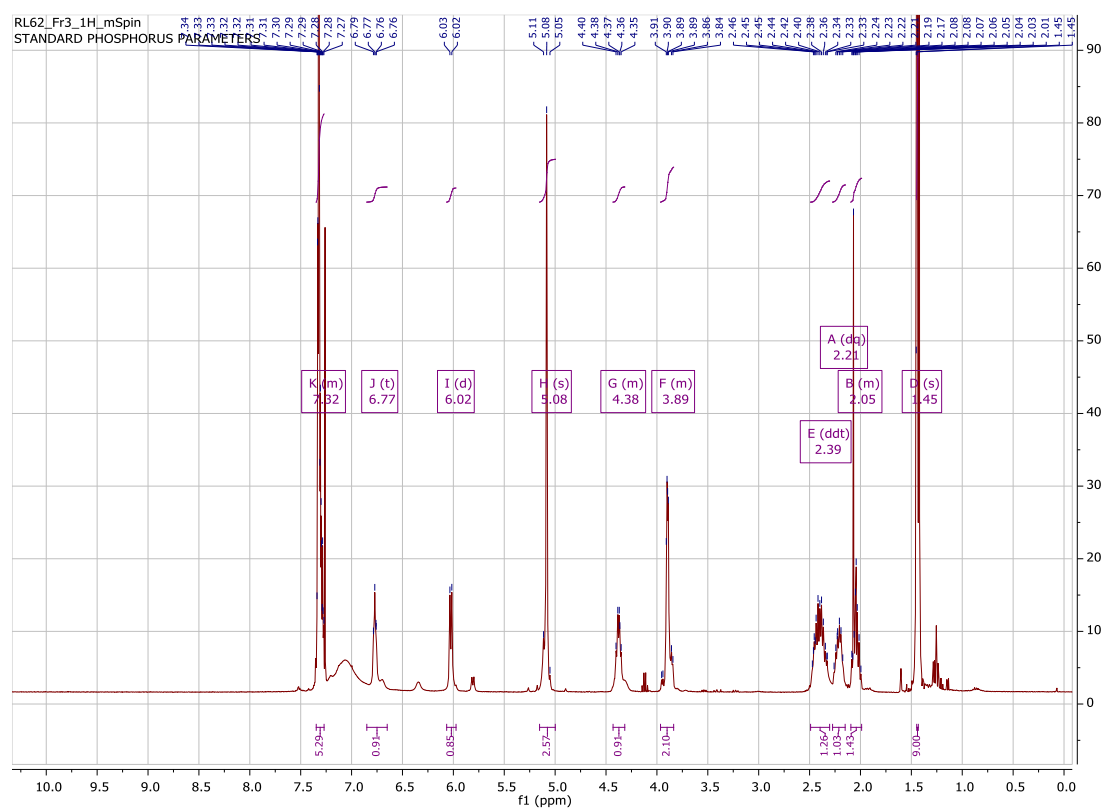
**Figure S7:**  $^{13}\text{C}$  NMR Spectrum of compound 2



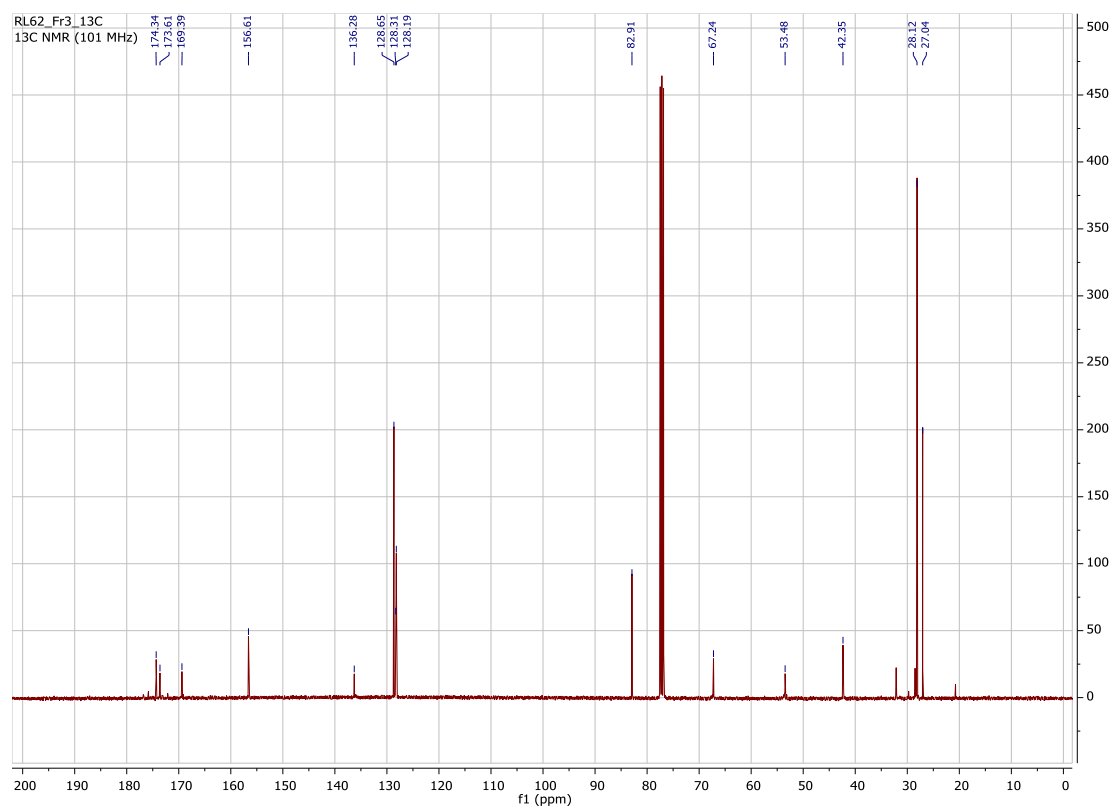
**Figure S8:**  $^1\text{H}$ ,  $^{13}\text{C}$  HSQC Spectrum of compound 2



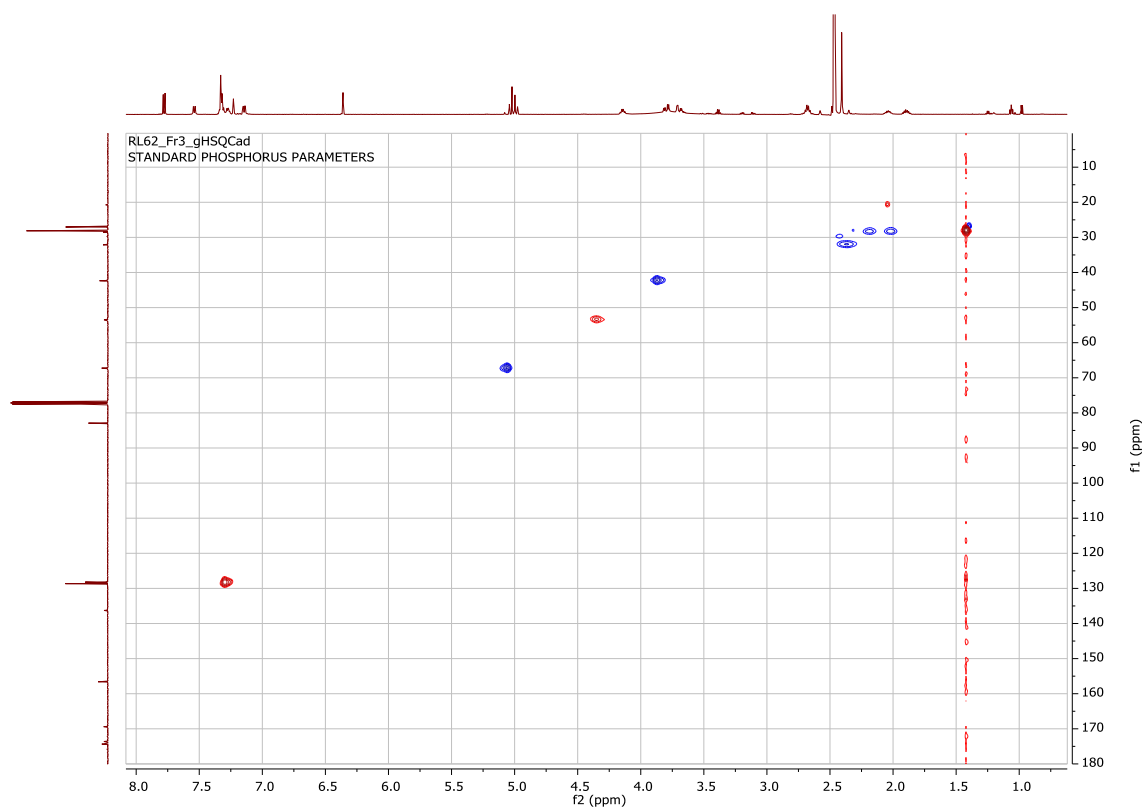
**Figure S9:**  $^1\text{H}$  NMR Spectrum of compound **2a**



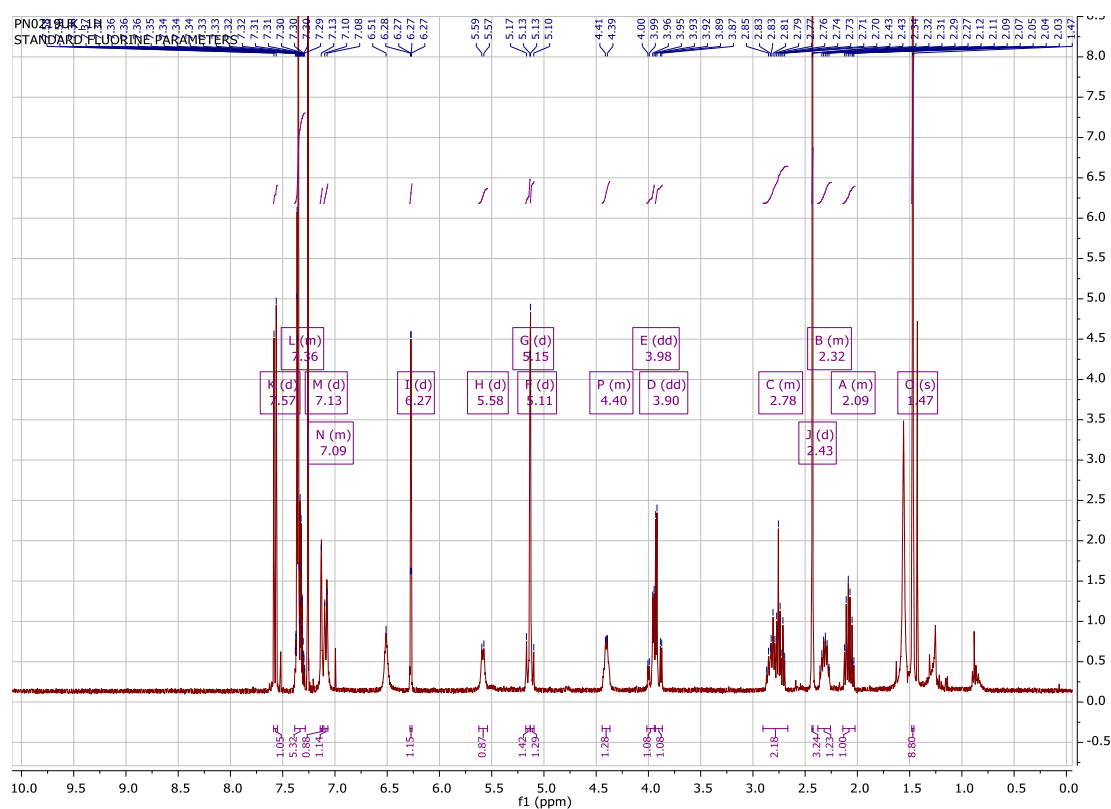
**Figure S10:**  $^{13}\text{C}$  NMR Spectrum of compound **2a**



**Figure S11:**  $^1\text{H}$ ,  $^{13}\text{C}$  HSQC Spectrum of compound 2a

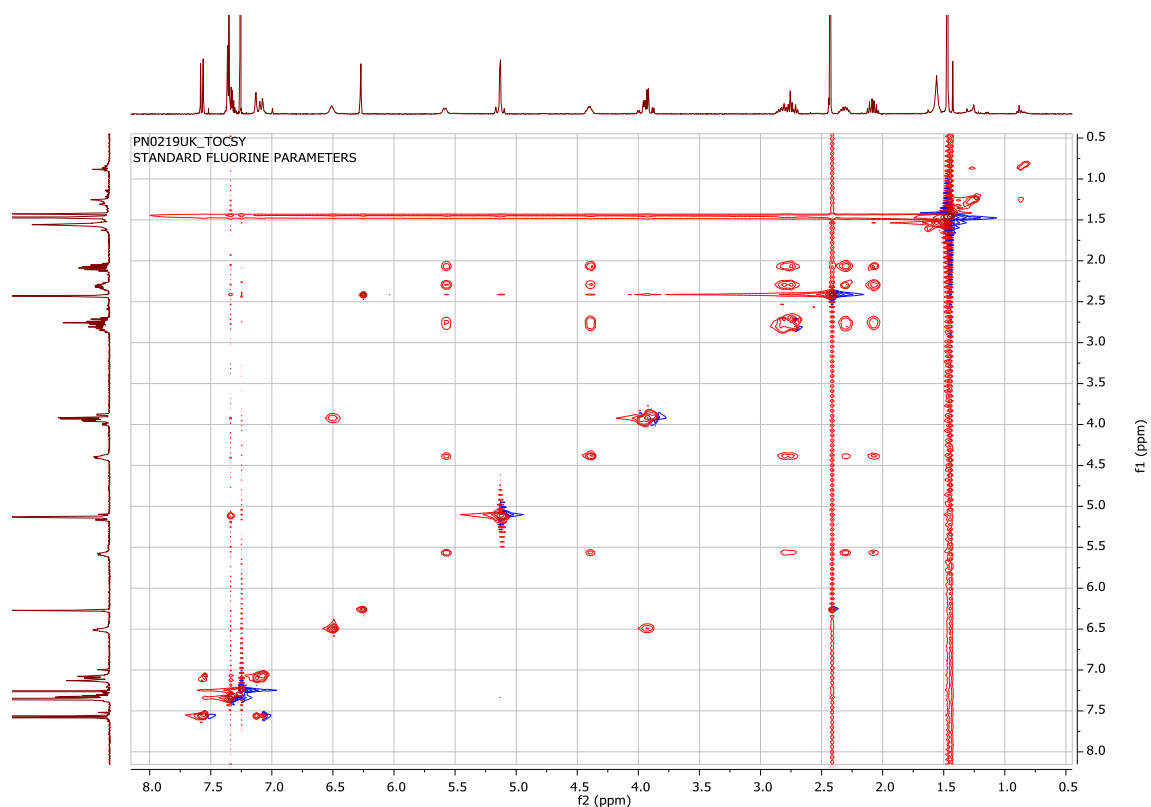


**Figure S12:**  $^1\text{H}$  NMR Spectrum of compound 3

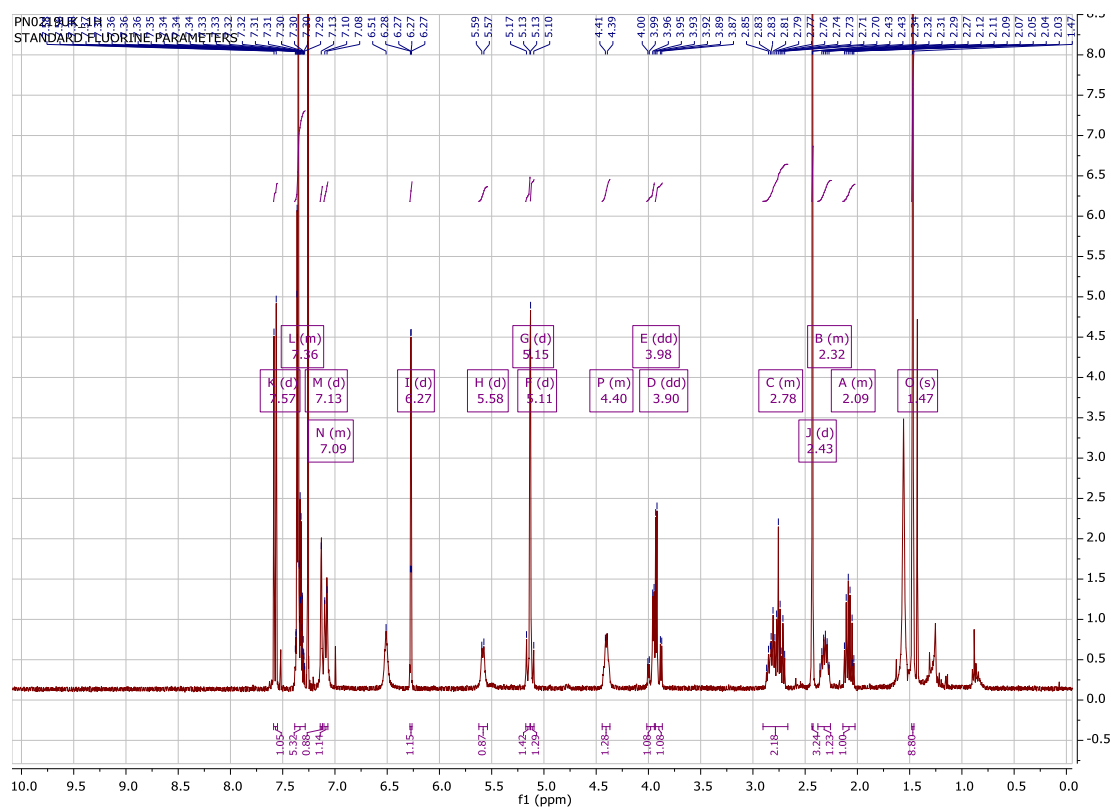




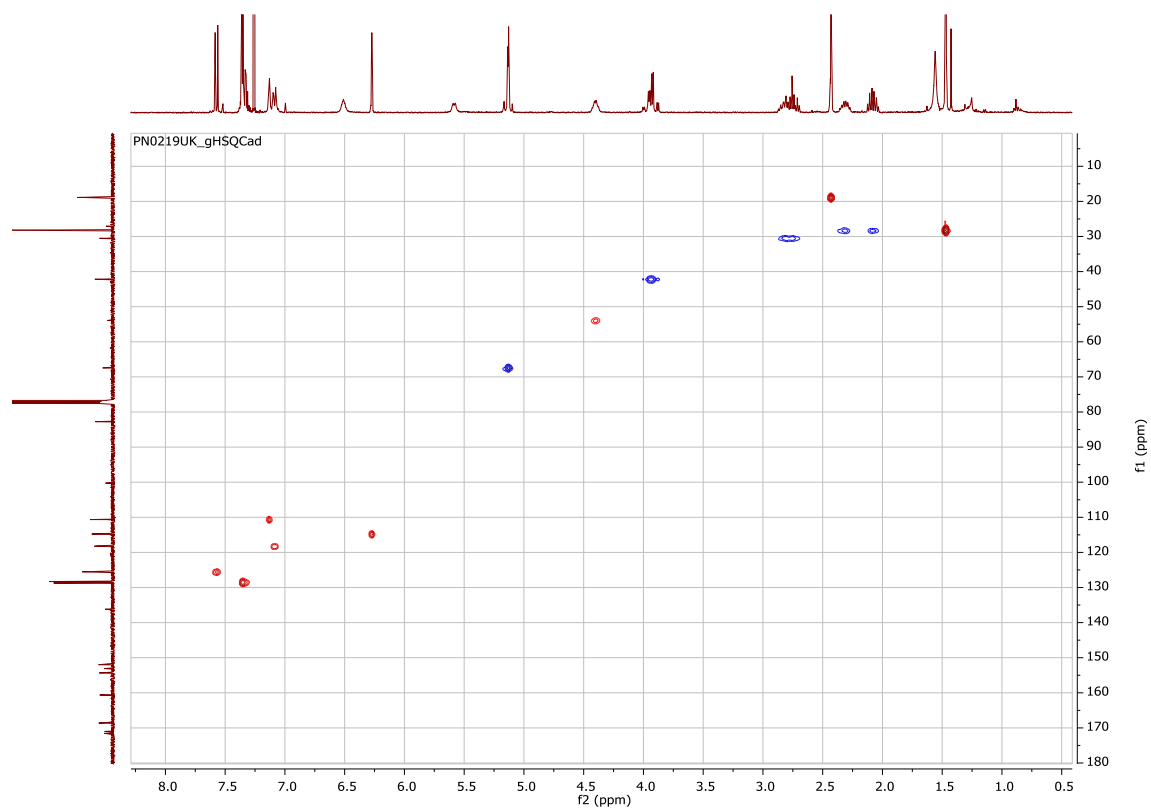
**Figure S13:** TOCSY Spectrum of compound **3**



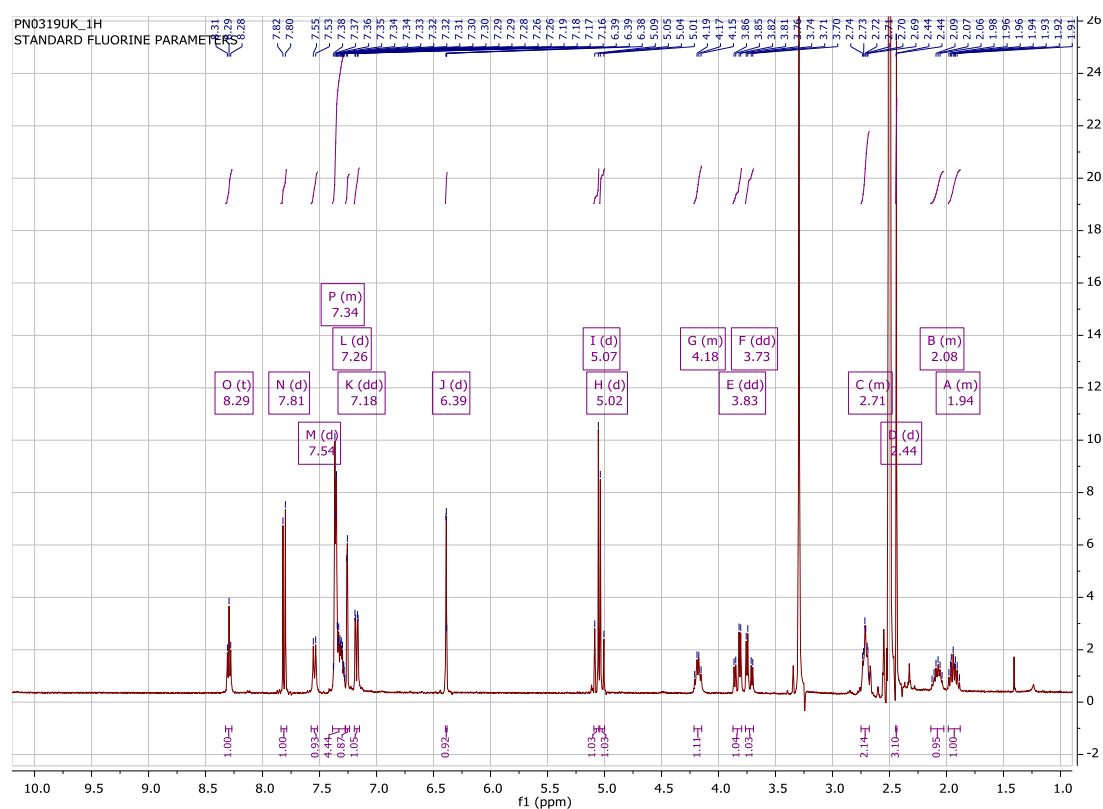
**Figure S14:**  $^{13}\text{C}$  NMR Spectrum of compound **3**



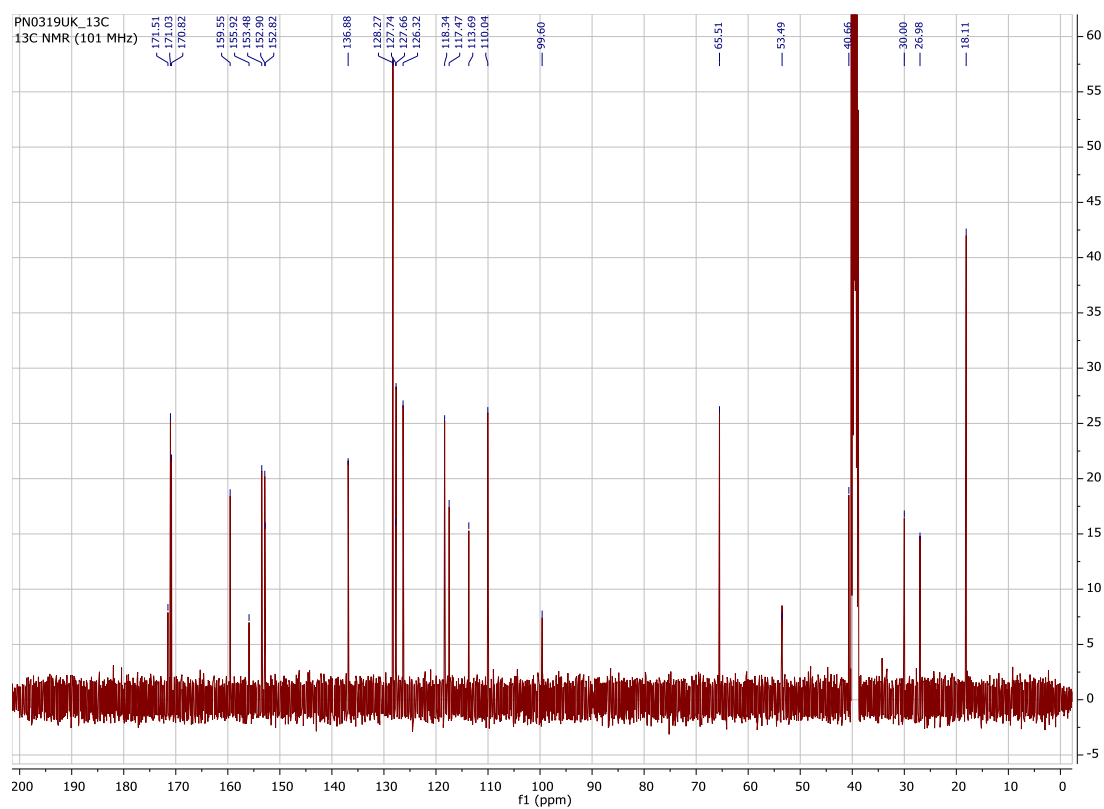
**Figure S15:**  $^1\text{H}$ ,  $^{13}\text{C}$  HSQC Spectrum of compound **3**



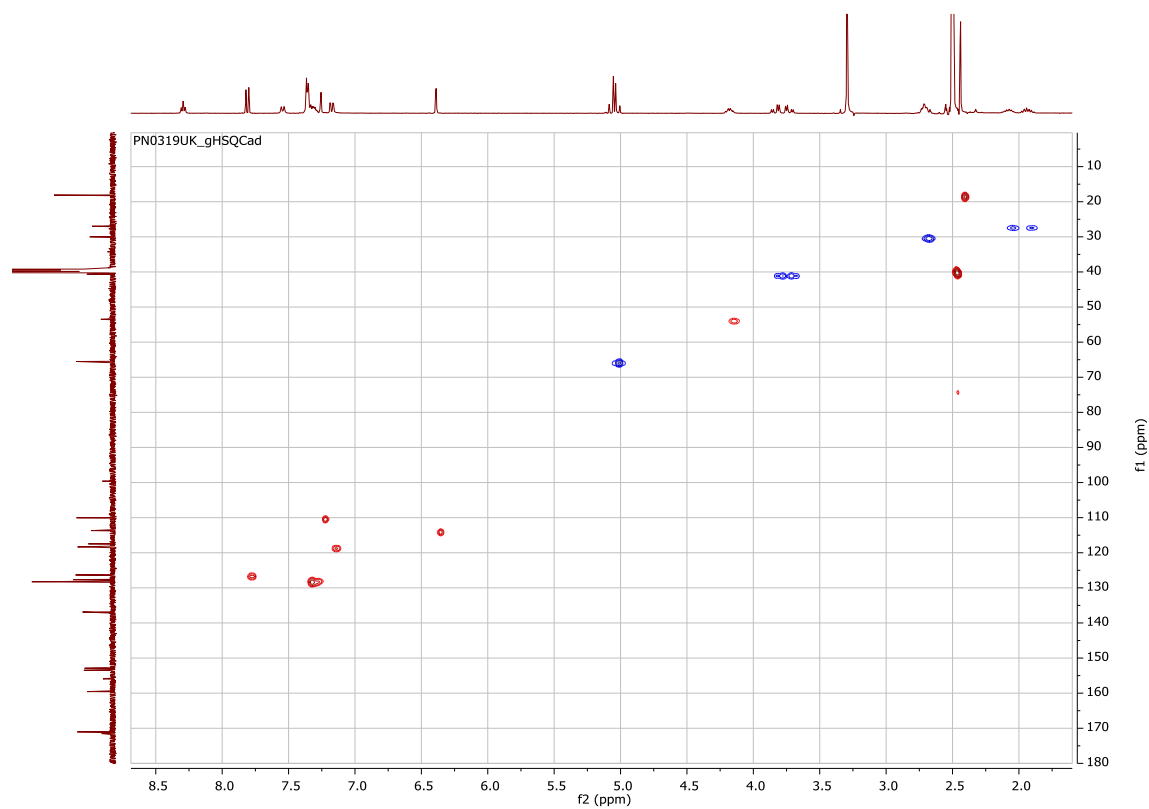
**Figure S16:**  $^1\text{H}$  NMR Spectrum of compound **4** (Z-Glu(HMC)-Gly-OH)



**Figure S17:**  $^{13}\text{C}$  NMR Spectrum of compound **4** (Z-Glu(HMC)-Gly-OH)



**Figure S18:**  $^1\text{H}$ ,  $^{13}\text{C}$  HSQC Spectrum of compound **4** (Z-Glu(HMC)-Gly-OH)



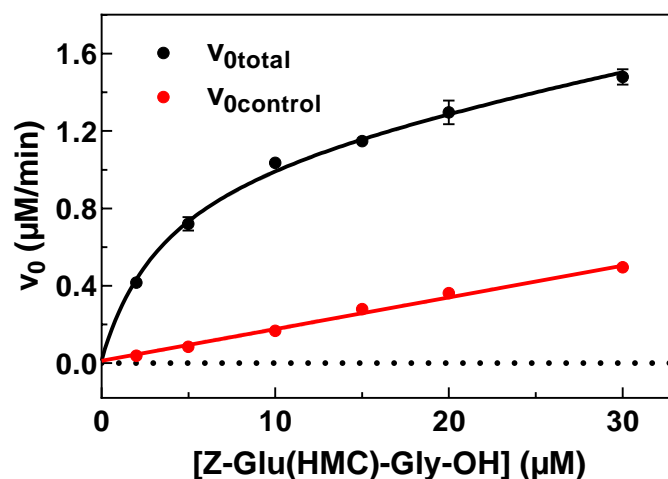


**Figure S19:** hTGase 2-catalysed hydrolysis of Z-Glu(HMC)-Gly-OH (**4**) at pH 8.0

Plots of  $v_{0\text{total}}=f([Z\text{-Glu(HMC)-Gly-OH}])$  and  $v_{0\text{control}}=f([Z\text{-Glu(HMC)-Gly-OH}])$  including the regression curves according to the global fit model of total and nonspecific binding as implemented in GraphPad Prism to determine the kinetic parameters of the enzymatic hydrolysis (see Materials and Methods section for a detailed description and see Figure 1 in the main article for the graph of  $v_{0\text{corr}}=f([Z\text{-Glu(HMC)-Gly-OH}])$ ). Data shown are mean values of three separate experiments each performed in duplicate. When not apparent, error bars are smaller than the symbols. Conditions: pH=8.0, 30 °C, 5% DMSO, 500 μM TCEP, 3 μg/mL hTGase 2.

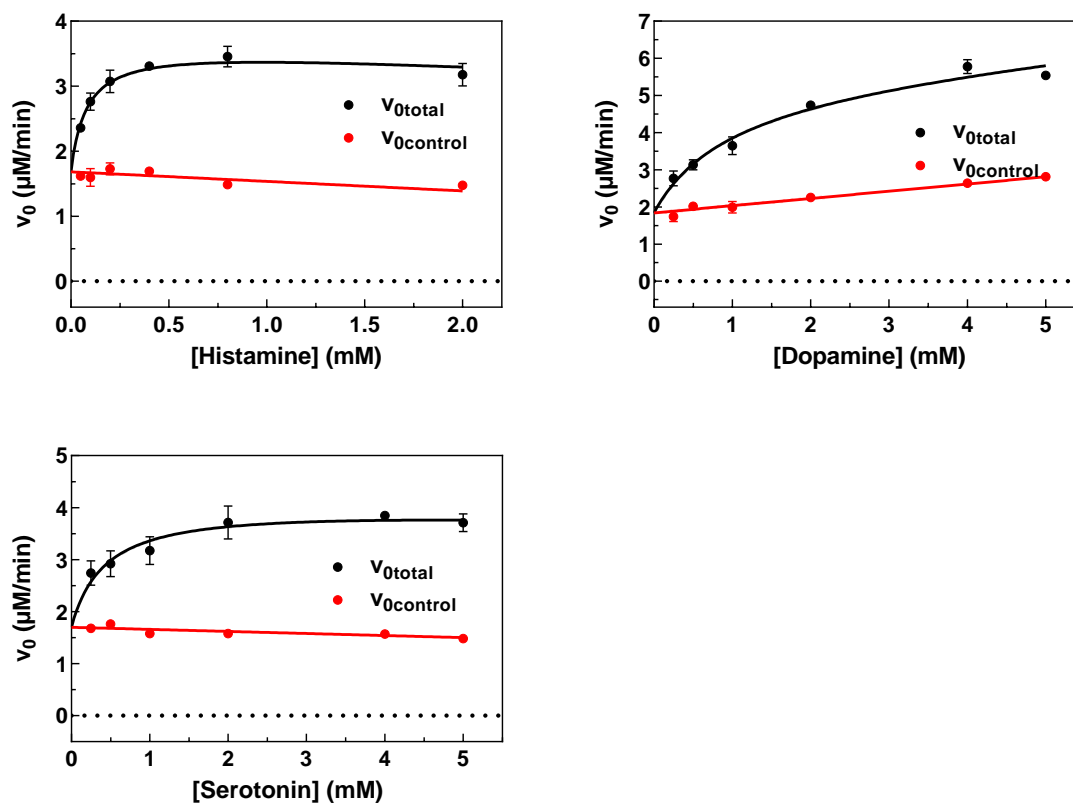
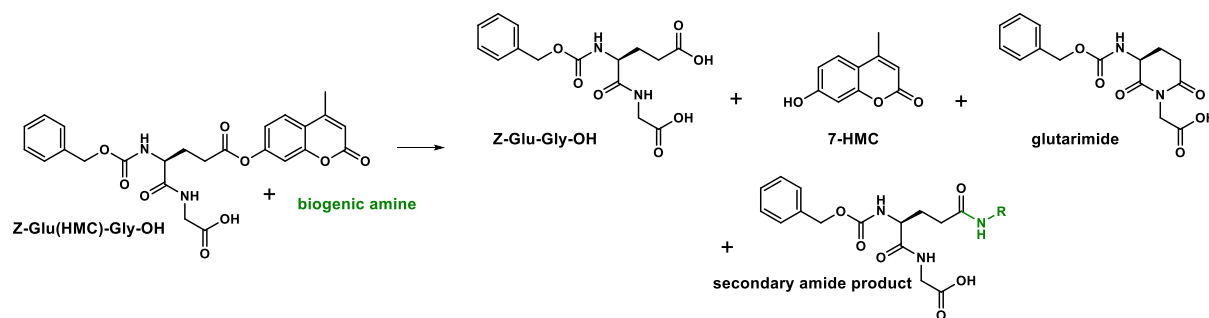


**Figure S20:** hTGase 2-catalysed incorporation of different biogenic amines into Z-Glu(HMC)-Gly-OH (4;  $c=100$  μM) at pH 8.0

Plots of  $v_{0total}=f([amine])$  and  $v_{0control}=f([amine])$  including the regression curves according to the global fit model of total and nonspecific binding as implemented in GraphPad Prism to determine the kinetic parameters of the enzymatic aminolysis (see Materials and Methods section for a detailed description and see Figure 2 in the main article for the graph of  $v_{0corr}=f([amine])$ ). Data shown are mean values of two independent experiments each performed in duplicate. When not apparent, error bars are smaller than the symbols. Conditions: pH=8.0 (100 mM MOPS was used, which ensures that the pH value is maintained over the entire range of amine concentrations), 30 °C, 5% DMSO, 500 μM TCEP, 0.6, 2 and 3 μg/mL of hTGase 2 for histamine, dopamine and serotonin, respectively. Substrate concentrations were adjusted within prior pilot experiments. Substrate inhibition did not occur at concentration as high as 5 mM such as for histamine. The high rates in the absence of amine ( $c=0$ ) are due to the TGase 2-catalysed and non-enzymatic hydrolysis of 4.



**Scheme S1:** Products of spontaneous and TGase 2-catalysed conversion of Z-Glu(HMC)-Gly-OH with biogenic amines.

### *General procedure for the LC-MS-analysis of the enzymatic aminolysis*

The assay mixtures (200  $\mu$ L) were diluted with 1.25% HOAc/CH<sub>3</sub>CN (800  $\mu$ L, LC-MS grade) and were kept on ice for 30 min to fully precipitate the protein. Subsequently, the mixture was centrifuged at 4  $^{\circ}$ C for 10 min (12.700 rpm). An aliquot of the supernatant (90  $\mu$ L) was transferred to a sample vial for UPLC-DAD-MS analysis (system from Waters: ACQUITY UPLC I-Class System including a ACQUITY UPLC PDA e $\lambda$ -Detector coupled to a Xevo TQ-S mass spectrometer) and water (30  $\mu$ L) was added. A volume of 1-5  $\mu$ L of those solutions was injected into the system. A Waters Acquity BEH C18 column (2.1x100 mm, 1.7  $\mu$ m particle size) was used as stationary phase. A binary gradient system of water (containing 0.1% CH<sub>3</sub>COOH) as solvent and CH<sub>3</sub>CN/CH<sub>3</sub>OH (1:1, containing 0.1% CH<sub>3</sub>COOH) as solvent B at a flow rate of 0.4 mL/min served as the eluent (gradient 15-65% B, 5 min).

### Analysis for histamine

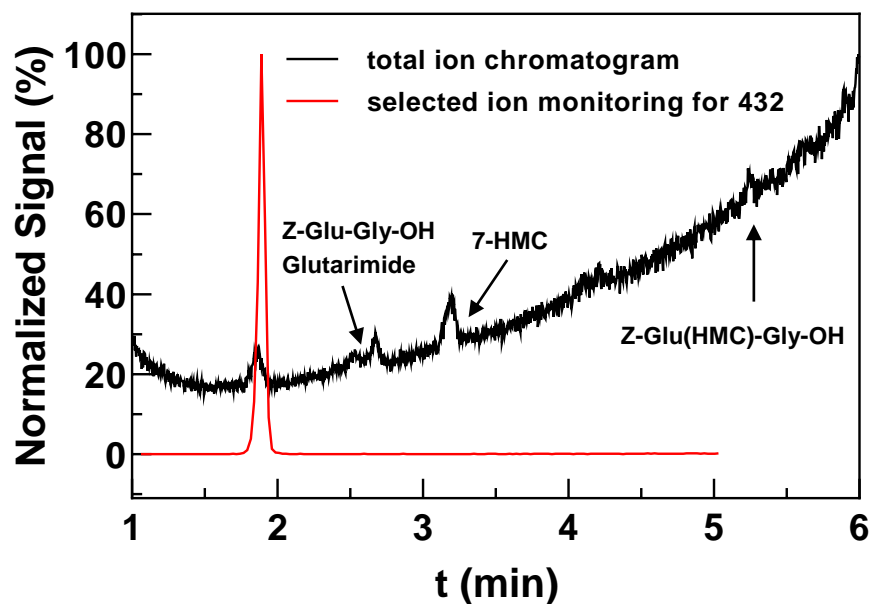


**Figure S21:** LC-MS analysis for the enzymatic aminolysis of **Z-Glu(HMC)-Gly-OH** with histamine. Conditions for the reaction mixture: pH 8.0, 30 °C, 5% DMSO, 500  $\mu$ M TCEP, 0.6  $\mu$ g/mL of hTGase 2, 2 mM of histamine, 100  $\mu$ M of **Z-Glu(HMC)-Gly-OH**, stop of the reaction after 1 h.

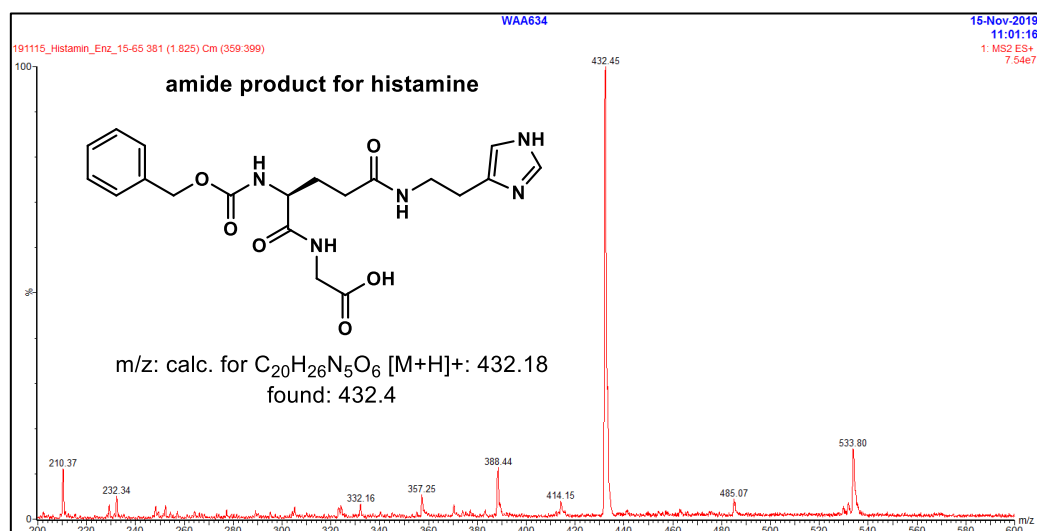


**Figure S22:** ESI(+) mass spectrum of the identified amide product for histamine.

## Analysis for dopamine

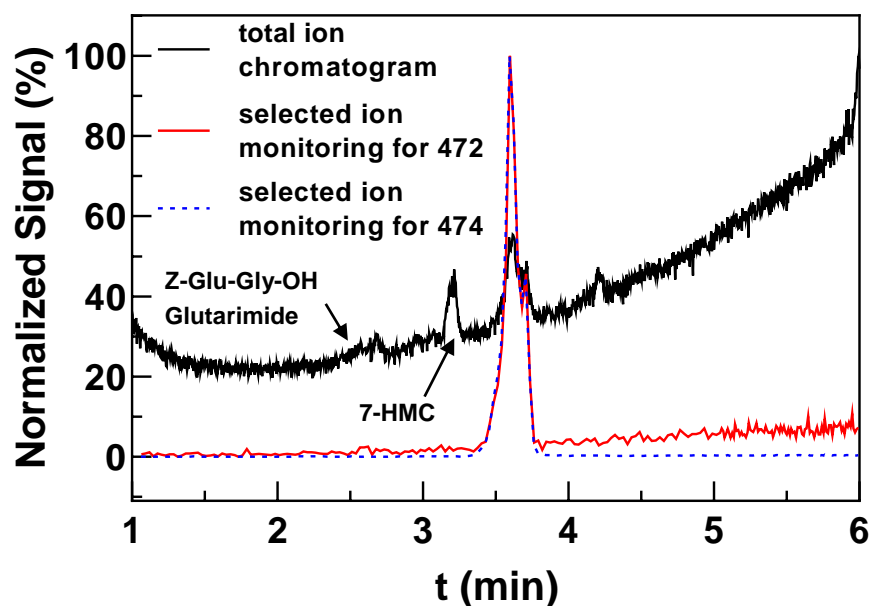


**Figure S23:** LC-MS analysis for the enzymatic aminolysis of Z-Glu(HMC)-Gly-OH with dopamine. Conditions for the reaction mixture: pH 8.0, 30 °C, 5% DMSO, 500  $\mu$ M TCEP, 2  $\mu$ g/mL of hTGase 2, 5 mM of dopamine, 100  $\mu$ M of Z-Glu(HMC)-Gly-OH, stop of the reaction after 1 h. The additional signal for m/z=472 amu is attributed to partial oxidation of the aminolysis product in the presence oxygen [1].

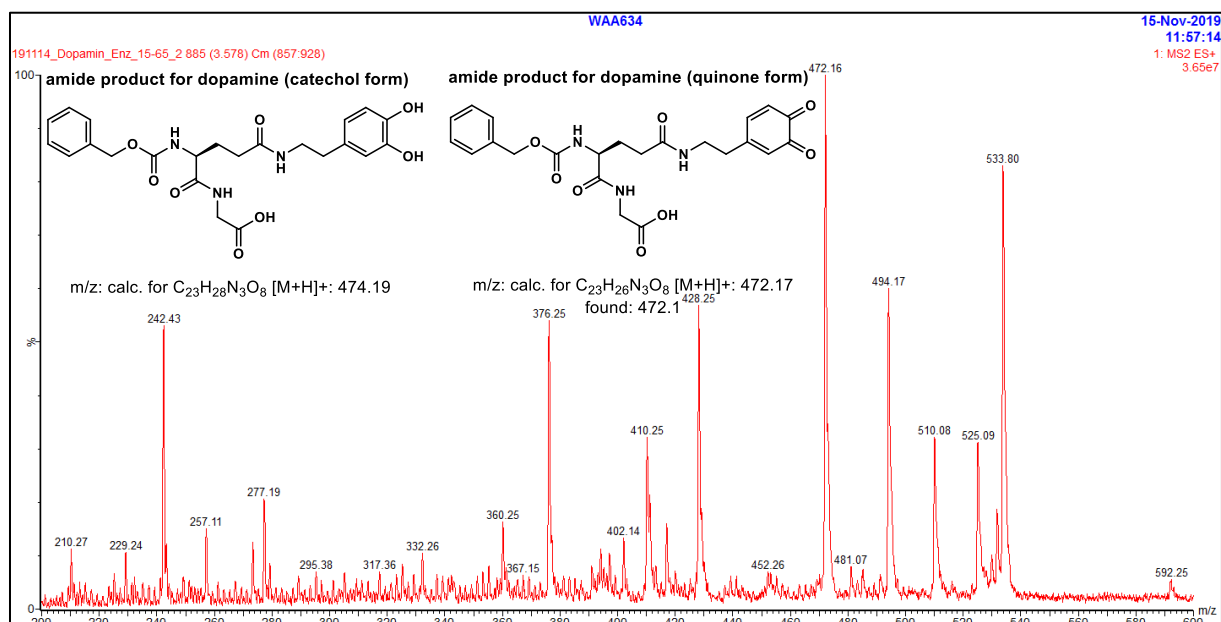


**Figure S24:** ESI(+) mass spectrum of the identified amide product for dopamine.



### Analysis for serotonin

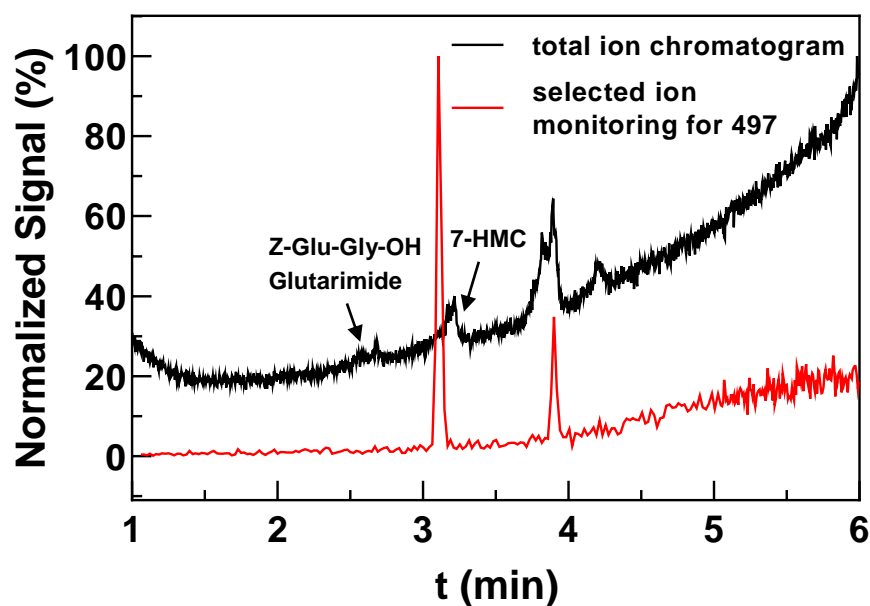


**Figure S25:** LC-MS analysis for the enzymatic aminolysis of **Z-Glu(HMC)-Gly-OH** with dopamine. Conditions for the reaction mixture: pH 8.0, 30 °C, 5% DMSO, 500  $\mu$ M TCEP, 3  $\mu$ g/mL of hTGase 2, 5 mM of serotonin, 100  $\mu$ M of **Z-Glu(HMC)-Gly-OH**, stop of the reaction after 1 h.

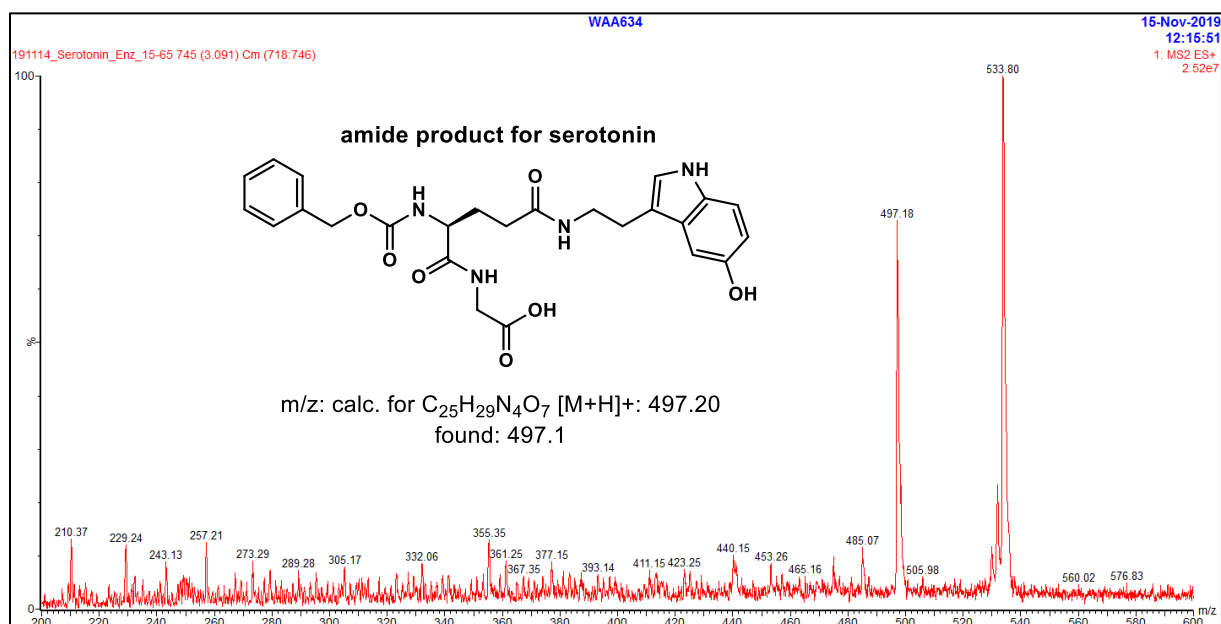


**Figure S26:** ESI(+) mass spectrum of the identified amide product for serotonin.

## Supplemental references

[1] J. Yang, M.A. Cohen Stuart, M. Kamperman, Jack of all trades: versatile catechol crosslinking mechanisms, *Chem. Soc. Rev.*, 43 (2014) 8271-8298.